

# Flood-Duration-Frequency modeling Application to ten catchments in Northern Iceland

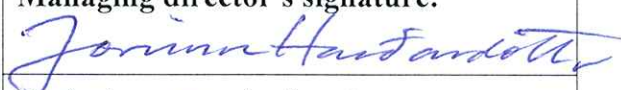
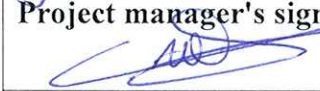
---

Philippe Crochet

# Flood-Duration-Frequency modeling. Application to ten catchments in Northern Iceland

---

Philippe Crochet, Icelandic Met Office

<b>Report no.:</b> VÍ 2012-006	<b>Date.:</b> June 2012	<b>ISSN:</b> 1670-8261	<b>Public</b> <input checked="" type="checkbox"/> <b>Restricted</b> <input type="checkbox"/> <b>Provision:</b>
<b>Report title / including subtitle</b> Flood-Duration-Frequency modeling. Application to ten catchments in Northern Iceland		<b>No. of copies:</b> 20 <b>Pages:</b> 50	<b>Managing director:</b> Jórunn Harðardóttir
<b>Author(s):</b> Philippe Crochet		<b>Project manager:</b> Philippe Crochet	<b>Project number:</b> 4812
<b>Project phase:</b>		<b>Case number:</b>	
<b>Report contracted for:</b> Vegagerðin			
<b>Prepared in cooperation with:</b>			
<b>Summary:</b> Streamflow data from ten hydrographic stations in Northern Iceland are used to develop flood-duration-frequency (QDF) curves, using the so-called continuous converging model. The QDF curves are equivalent to the well known intensity-duration-frequency (IDF) curves used in extreme rainfall modeling, except that they are applied to discharge data which is the variable of interest. QDF curves give a complete description of the flood dynamics of a basin and allow to directly derive the $T$ -year flood peak discharge of any duration $D$ with a unique and straightforward formula. Results obtained so far indicate that the approach adopted in this study looks promising for deriving QDF curves and complement the regional flood frequency analysis recently developed at the Icelandic Meteorological Office (IMO) for estimating the $T$ -year flood at ungauged catchments. The QDF curves will also be useful for deriving extreme flood statistics of any duration $D$ from simulated daily discharge series made with the WaSiM-ETH distributed hydrological model used at IMO and will thus enhance its usefulness.			
<b>Keywords:</b> Iceland, flood duration frequency analysis		<b>Managing director's signature:</b> 	
		<b>Project manager's signature:</b> 	
		<b>Reviewed by:</b> Tómas Jóhannesson, Ásdís Helgadóttir	



# Contents

<b>1</b>	<b>Introduction</b> .....	8
<b>2</b>	<b>Flood-Duration-Frequency modeling</b> .....	8
2.1	QDF model I.....	8
2.2	QDF model II.....	10
2.3	QDF model refinements .....	11
2.4	Maximum flood duration .....	12
2.5	Flood probability distribution function and parameter estimation.....	12
<b>3</b>	<b>Data</b> .....	13
3.1	River basins .....	13
3.2	Streamflow data .....	16
<b>4</b>	<b>Results</b> .....	16
<b>5</b>	<b>Conclusion and future research</b> .....	27
<b>6</b>	<b>Acknowledgements</b> .....	27
<b>7</b>	<b>References</b> .....	28
	<b>Appendix-I: Estimated GEV/PWM cumulative distribution functions (CDF) of annual maximum instantaneous flood using QDF models I and III.....</b>	29
	<b>Appendix-II: Estimated dimensionless parent cumulative distribution functions (CDF), <math>q(T)</math>, using QDF models II and IV .....</b>	40



## Abstract

Streamflow data from ten hydrographic stations in Northern Iceland are used to develop flood-duration-frequency (QDF) curves, using the so-called continuous converging model. The QDF curves are equivalent to the well known intensity-duration-frequency (IDF) curves used in extreme rainfall modeling, except that they are applied to discharge data which is the variable of interest. QDF curves give a complete description of the flood dynamics of a basin and allow to directly derive the  $T$ -year flood peak discharge of any duration  $D$  with a unique and straightforward formula. Results obtained so far indicate that the approach adopted in this study looks promising for deriving QDF curves and complement the regional flood frequency analysis recently developed at the Icelandic Meteorological Office (IMO) for estimating the  $T$ -year flood at ungauged catchments. The QDF curves will also be useful for deriving extreme flood statistics of any duration  $D$  from simulated daily discharge series made with the WaSiM-ETH distributed hydrological model used at IMO and will thus enhance its usefulness.

# 1 Introduction

Various water resources applications require the calculation of the so-called  $T$ -year flood peak discharge, i.e. the flood peak magnitude with return period of  $T$ -years. Such information is usually needed for the design of bridges or dams and in hydrological applications e.g. reservoir operation and dam safety analysis. Often, such studies are limited to the analysis of annual maximum instantaneous flood statistics or annual maximum daily flood statistics. This information is not always sufficient to fully describe the flood dynamics and analysing flood discharge corresponding to various durations ( $D$ ) may also be important. Sometimes, only daily streamflow series are available which may be insufficient temporal resolution for small catchments.

Recently, Atladóttir *et al.* (2011) made an attempt to estimate the  $T$ -year flood at poorly gauged and ungauged catchments in the West-fjords using the WaSiM-ETH distributed hydrological model. Despite the intrinsic advantages of this model, one limitation is the temporal resolution of the simulated streamflow series,  $D=24\text{h}$ , imposed by the available input meteorological information. In practise, some sort of downscaling would be needed for applications requiring sub-daily or even instantaneous  $T$ -year flood estimates.

The problem of data resolution and multi-duration analysis of extreme floods is explicitly adressed here. A methodology is presented for deriving Flood-Duration-Frequency (QDF) curves and estimating the  $T$ -year flood of any duration  $D$ . The selected approach builds on the so-called continuous converging model (Javelle *et al.*, 2002; Javelle *et al.*, 2003). The report is organized as follows. Section 2 describes the general methodology. Section 3 presents the data used in the study and Section 4 presents the derivation of the QDF curves for the selected river basins. Finally, Section 5 concludes the report.

## 2 Flood-Duration-Frequency modeling

The Flood-Duration-Frequency (QDF) modeling is similar to the Intensity-Duration-Frequency (IDF) curves commonly used in extreme rainfall modeling (see for instance Eliasson, 2000). The idea is to provide a description of flood magnitude as a continuous function of both return period ( $T$ ) and duration ( $D$ ) and give a more comprehensive picture of the dynamics or regime of extreme floods for a given basin. First, averaged discharge series are computed for different durations,  $D$ , their annual maxima extracted and the quantiles, denoted  $Q(D, T)$ , estimated by fitting an appropriate extreme value distribution. The QDF methodology attempts to describe the relationship between the different distributions corresponding to different durations. For a given year, the annual maxima of different durations do not necessarily correspond to the same flood event.

### 2.1 QDF model I

The two underlying hypothesis behind the QDF modeling approach of Javelle *et al.* (2002) are that i) the distributions of annual maximum floods for the different durations,  $D$ , converge towards the same point  $P$  for small return periods and ii) for a given return period,  $T$ , the evolution of the quantile  $Q(D, T)$  as a function of  $D$  can be described by a hyperbolic form:



$$Q(D, T) = \frac{Q(D=0, T) - P}{1 + D/\Delta} + P, \quad (1)$$

where  $Q(D=0, T)$  is the instantaneous flood quantile,  $\Delta$  is a parameter with unit of time describing the shape of the hyperbolic form and related to the flood dynamics and  $P$  is the limit of the function when  $D$  tends to infinity. A large value of  $\Delta$  corresponds to slow and smoothed floods whereas a small value of  $\Delta$  corresponds to fast and sharp floods. The parameter  $\Delta$  can thus be seen as being characteristic for the basin in question. This function can be simplified by taking  $P = 0$  with a small loss of performance only:

$$Q(D, T) = \frac{Q(D=0, T)}{1 + D/\Delta}. \quad (2)$$

If the characteristic basin parameter  $\Delta$  is known, then the instantaneous flood quantile  $Q(D=0, T)$  can be derived from the flood quantile of any duration  $D$  and return period  $T$ ,  $Q(D, T)$ , as follows:

$$Q(D=0, T) = Q(D, T)(1 + D/\Delta). \quad (3)$$

This property may be used to estimate the parameter  $\Delta$ . First, each available experimental annual maximum streamflow series corresponding to duration  $D_i$ ,  $Q(D_i, j)$ , is scaled:

$$x(D_i, j, \delta) = Q(D_i, j)(1 + D_i/\delta), \quad (4)$$

and  $\Delta$  is estimated as the optimum value of  $\delta$  that minimizes the dispersion of  $x(D_i, j, \delta)$ :

$$\Delta = \delta_{optimum} = \text{Min}(Err(\delta)), \quad (5)$$

where

$$Err(\delta) = \frac{1}{M} \frac{1}{N} \sum_{j=1}^M \sum_{i=1}^N \left[ \frac{x(D_i, j, \delta) - E[x(j, \delta)]}{E[x(j, \delta)]} \right]^2, \quad (6)$$

and  $E[x(j, \delta)]$  is the mean experimental scaled value for year  $j$  over all durations  $D_i$

$$E[x(j, \delta)] = \frac{1}{N} \sum_{i=1}^N x(D_i, j, \delta). \quad (7)$$

$N$  is the number of analysed durations  $D_i$  ( $i=1, \dots, N$ ) and  $M$  is the sample size for each duration (number of years).

Once the parameter  $\Delta$  has been found, the parameters of the probability distribution function of  $Q(D=0)$  are estimated by fitting an appropriate extreme value distribution to  $E[x(j, \delta_{optimum})]$

and the quantiles  $Q(D, T)$  for any duration  $D$  and return period  $T$  are estimated by Eq. (2). In this work, the GEV distribution fitted by the method of probability weighed moments (PWM) (Hosking *et al.*, 1985a) will be used (see also Crochet, 2012).

This approach, described by a unique formula, is a quick and straightforward way to derive the distribution of annual maximum flood for any duration. In particular, this method is attractive for estimating the distribution of annual maximum instantaneous flood which is often required in flood design studies and not always available from flow measurements or simulations. Hydrological models, in particular, simulate streamflow averaged over a duration of a few hours or a day, like for instance the WaSiM-ETH distributed hydrological model used at IMO.

## 2.2 QDF model II

More recently, Javelle *et al.*(2003) proposed a refinement of the Javelle *et al.*(2002) method presented above, allowing a more robust fitting of the parameter  $\Delta$ . The two main hypothesis are:

i) The different distributions are invariant when normalized by their mean  $\mu(D)$ :

$$Q(D, T) = \mu(D)q(T), \quad (8)$$

where  $q(T)$  is a dimensionless parent distribution with a mean of unity and is equivalent to the growth curve in regional index flood procedures (see Crochet, 2012).

ii) The scaling factor  $\mu(D)$  can be modeled as a continuous function of  $D$ , similarly to what was previously done with  $Q(D, T)$  (see Eq. (2)):

$$\mu(D) = \frac{\mu}{1 + D/\Delta}, \quad (9)$$

where  $\mu$  and  $\Delta$  have to be estimated. The parameter  $\Delta$  has a unit of time and is equivalent to the  $\Delta$  parameter defined in Eq. (2) and  $\mu$  is the mean of the annual maximum instantaneous ( $D = 0$ ) flood distribution. The  $Q(D, T)$  quantile can then be modeled by:

$$Q(D, T) = \frac{\mu}{1 + D/\Delta}q(T), \quad (10)$$

and the annual maximum instantaneous flood quantile is given by:

$$Q(D = 0, T) = \mu q(T). \quad (11)$$

The optimal model parameters  $\Delta$  and  $\mu$  are calculated, considering that:

$$\mu = \mu(D)(1 + D/\Delta). \quad (12)$$

In other words, the sample mean  $\mu(D)$  multiplied by the coefficient  $(1 + D/\Delta)$  should converge towards the same value  $\mu$ , for all  $D$ . The following new optimization procedure was suggested

by Javelle *et al.*(2003) and is assumed more robust than the earlier one described in previous sub-section. For each duration  $D_i$  and a set of values  $\delta$ , the following quantities are calculated:

$$\mu_q(D_i, \delta) = \mu(D_i)(1 + D_i/\delta), \quad (13)$$

$$E[\mu_q(D_i, \delta)] = \frac{1}{N} \sum_{i=1}^N \mu_q(D_i, \delta), \quad (14)$$

$$\text{Var}\{\mu_q(D_i, \delta)\} = \frac{1}{N} \sum_{i=1}^N (\mu_q(D_i, \delta) - E[\mu_q(D_i, \delta)])^2, \quad (15)$$

where  $N$  is the number of analysed durations  $D_i$  ( $i=1, \dots, N$ ). The parameter  $\Delta$  is estimated as the optimum value of  $\delta$  that minimizes the variance of  $\mu_q(D_i, \delta)$  ( $\text{Var}\{\mu_q(D_i, \delta)\}$ ) and  $\mu$  is then estimated from Eqs. (13) and (14).

The dimensionless parent distribution  $q(T)$  is then fitted with the regional GEV/PWM algorithm (Hosking *et al.*, 1985b) using the normalized experimental flood samples  $q(D_i, j)$  for each duration  $D_i$ :

$$q(D_i, j) = Q(D_i, j) \frac{1 + D_i/\Delta}{\mu} \Rightarrow q(D_i, T) \Rightarrow q(T). \quad (16)$$

The regional GEV/PWM algorithm has recently been used in Crochet (2012) on river basins in Northern Iceland for estimating regional flood frequency distributions on ungauged basins. The same algorithm will be employed here but applied to  $q(D_i, j)$ .

### 2.3 QDF model refinements

In order to refine the methodologies presented in sections 2-1 and 2-2 and allow more flexibility in the modeling, the following two additional QDF models are proposed and tested:

i) QDF model III is defined by modifying QDF model I as follows:

$$Q(D, T) = \frac{Q(D=0, T)}{(1 + (D/\Delta)^\Theta)}, \quad (17)$$

with  $0 < \Theta \leq 1$  and the same optimization method defined in section 2-1 is used except that one more parameter ( $\Theta$ ) needs to be fitted. It follows that the annual maximum instantaneous flood quantile is estimated by:

$$Q(D=0, T) = Q(D, T)(1 + (D/\Delta)^\Theta), \quad (18)$$

ii) QDF model IV is defined by modifying QDF model II as follows:

$$Q(D, T) = \frac{\mu}{1 + (D/\Delta)^\Theta} q(T), \quad (19)$$

with

$$\mu(D) = \frac{\mu}{1 + (D/\Delta)^\Theta}, \quad (20)$$

with  $0 < \Theta \leq 1$  and the same optimization method defined in section 2-2 is used but one additional parameter,  $\Theta$ , needs to be fitted. The annual maximum instantaneous flood quantile is estimated by:

$$Q(D = 0, T) = \mu q(T), \quad (21)$$

where the dimensionless parent distribution  $q(T)$  is fitted as for QDF model II by the regional GEV/PWM method, using the normalized experimental flood samples  $q(D_i, j)$  for each duration  $D_i$ :

$$q(D_i, j) = Q(D_i, j) \frac{1 + (D_i/\Delta)^\Theta}{\mu} \Rightarrow q(D_i, T) \Rightarrow q(T). \quad (22)$$

## 2.4 Maximum flood duration

The maximum flood duration  $D_{max}$  to be used in the QDF model calibration is basin-dependent. It should be of the same order of magnitude as the average duration of flood events. Following Javelle *et al.* (2003),  $D_{max}$  is estimated by calculating the time during which half of the peak value of each flood event is continuously exceeded and then by taking the median of this duration  $d_{med}$  and by defining discrete durations  $D_i$  as follows (see Javelle *et al.*, (2003) for more details):

$$D_i = \begin{cases} 1, 2, 3, 4 & \text{if } d_{med} < 3 \text{ days} \\ 1, 2, 3, 4, 5, 6 & \text{if } d_{med} = 3 \text{ days} \\ 1 + \text{int}(\frac{i-1}{4} d_{med}) & \text{if } d_{med} > 3 \text{ days, } 1 \leq i \leq 7, \end{cases} \quad (23)$$

where  $D_i$  is an integer number of days and  $\text{int}()$  represents the integer value function.

## 2.5 Flood probability distribution function and parameter estimation

As mentioned above, the GEV distribution estimated by the method of probability weighted moments (PWM), (Hosking *et al.*, 1985a), is used in this study to model both the individual flood distributions for each duration,  $Q(D, T)$ , and the dimensionless parent distribution,  $q(T)$ , (Hosking *et al.*, 1985b). The GEV Cumulative Distribution Function (CDF) is:

$$G(q) = \text{Prob}(Q \leq q) = \begin{cases} \exp[-(1 - \kappa(\frac{q-\xi}{\alpha}))^{1/\kappa}] & \text{if } \kappa \neq 0 \\ \exp[-\exp(-\frac{q-\xi}{\alpha})] & \text{if } \kappa = 0, \end{cases} \quad (24)$$

where  $Q$  is a random variable,  $q$  a possible value of  $Q$ ,  $\kappa$  is the shape parameter,  $\varepsilon$  the location parameter and  $\alpha$  the scale parameter. This distribution combines into a single form the three types of limiting distributions for extreme values. Extreme value distribution Type 1 ( $\kappa=0$ ), Type 2 ( $\kappa<0$ ) and Type 3 ( $\kappa>0$ ). The case with  $\kappa=0$  corresponds to the Gumbel distribution. The  $p$ -th quantile which is the value  $q_p$  with cumulative probability  $p$ , ( $G(q_p) = \text{Prob}(Q \leq q_p) = p$ ), is estimated as follows:

$$\hat{q}_p = \begin{cases} \varepsilon + \frac{\alpha}{\kappa}(1 - [-\ln(p)]^\kappa) & \text{if } \kappa \neq 0 \\ \varepsilon - \alpha \ln(-\ln(p)) & \text{if } \kappa = 0, \end{cases} \quad (25)$$

The  $p$ -th quantile is associated to the return period  $T = 1/(1 - p)$  and can also be written as follows:

$$\hat{q}(T) = \begin{cases} \varepsilon + \frac{\alpha}{\kappa}(1 - [-\ln(1 - 1/T)]^\kappa) & \text{if } \kappa \neq 0 \\ \varepsilon - \alpha \ln(-\ln(1 - 1/T)) & \text{if } \kappa = 0. \end{cases} \quad (26)$$

The calculation of  $\kappa$ ,  $\varepsilon$  and  $\alpha$  is not given here as it can be found in Hosking *et al.*, 1985a and 1985b.

## 3 Data

### 3.1 River basins

A set of ten river catchments located in Northern Iceland was selected for this study. These catchments were also studied in Crochet (2012) to develop a regional flood frequency analysis for ungauged catchments in Northern Iceland. The catchments location is presented in Figure 1 with the topographic map and in Figure 2 with the mean annual precipitation map (Crochet *et al.*, 2007). This region is characterised by complex topography and consequently by a large precipitation variability. Table 1 gives the mean altitude and mean area-averaged precipitation for the catchments.

Gauging station	Name	Area (km <sup>2</sup> )	Mean elevation (m a.s.l)	Precipitation (71-00) (mm)
VHM-10	Svartá	398	535	813
VHM-12	Haukadalsá	167	404	1773
VHM-198	Hvalá	195	403	1971
VHM-19	Dynjandisá	37	529	3018
VHM-200	Fnjóská	1096	715	1312
VHM-204	Vatnsdalsá	103	456	2937
VHM-38	Þverá	43	427	1761
VHM-51	Hjaltadalsá	296	730	1711
VHM-92	Bægisá	39	934	1928
VHM-45	Vatnsdalsá	456	553	846

*Table 1. Main characteristics of the river basins.*

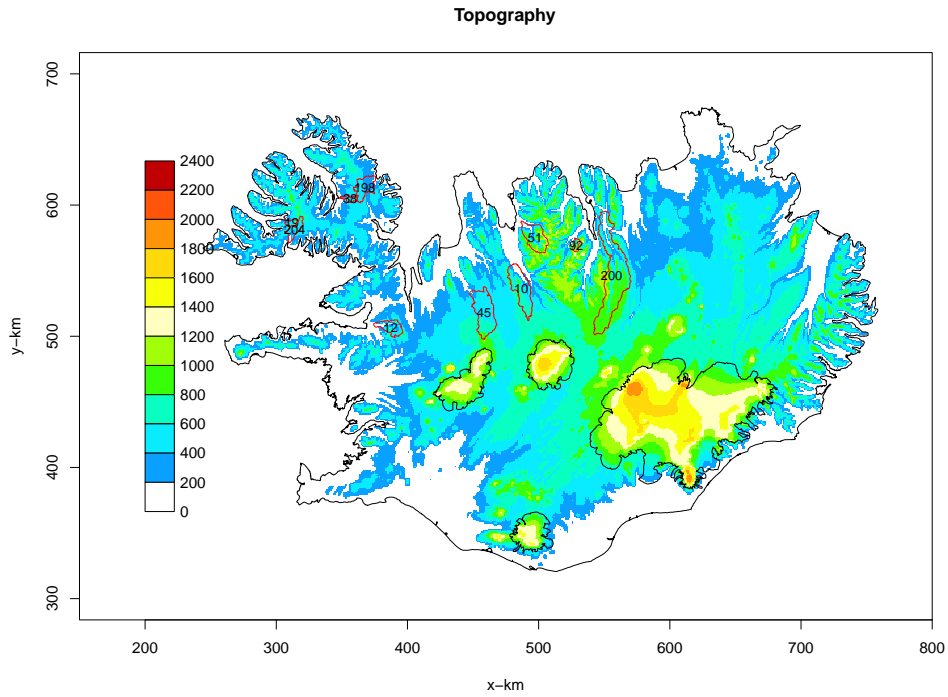


*Figure 1. Topography (m a.s.l) and location of catchments.*

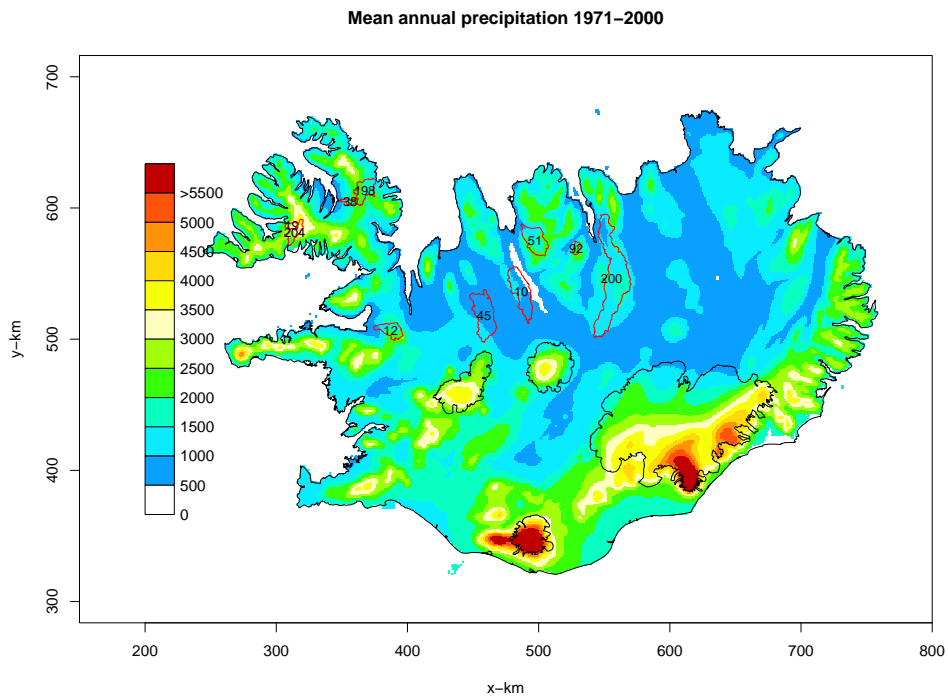


*Figure 2. Mean annual precipitation (mm) for the standard period 1971–2000 and location of catchments.*

## 3.2 Streamflow data

In this study, daily discharge series and monthly maximum instantaneous discharge series were used. Annual maximum instantaneous flood discharge series were extracted from the monthly maxima for each hydrological year defined from the 1st of September to the 31st of August and years with more than four months missing were omitted. Daily streamflow series were used to calculate average streamflow series of duration  $D \geq 24\text{h}$ , using a moving window of 24h, and the annual maximum was extracted. Years with more than 120 days of missing data were omitted. The annual maxima series for  $D \geq 24\text{h}$  do not give the true annual maxima of duration  $D$  because they were built from daily series which are only known for a fixed 24h window defined from 00UTC to 00UTC. The true annual maximum of duration  $D$  can only be calculated if continuous instantaneous measurements are available. However, as  $D$  increases, the estimated maxima converges towards the true maxima. Finally, only the longest continuous period with no missing years is selected from the annual maximum series of each basin.

Depending on the basin under consideration, the year and duration  $D$ , the annual maximum flood discharge can take place during different seasons. Spring floods are associated with snowmelt, winter floods can originate from a mixture of snowmelt and rainfall and autumn floods are usually associated with heavy rain. These different flood-generating mechanisms may lead to different types of floods which should from a dynamical and statistical point of view be analysed separately. However, for the sake of simplicity and because of time limitations, the annual maximum flood will be used in this study without distinguishing between the origin of the generating mechanism.

## 4 Results

This section presents the results of the QDF analysis. Two case studies are considered. First, the four QDF models presented in Section 2 are calibrated using only floods of durations  $D \geq 24\text{h}$ , and then by including the instantaneous floods ( $D = 0$ ). This is done in order to test the capacity of the QDF models to estimate instantaneous flood statistics when only daily streamflow series are available. In the results presented here for QDF models III and IV, the parameter  $\Theta$  was optimized considering the following range :  $0.2 \leq \Theta \leq 1$ .

Daily streamflow series were used to calculate the median flood duration  $d_{med}$  and Eq. (23) was used to define the maximum flood duration  $D_{max}$ . However, in this study, the number of discrete durations was not limited to 7 as in Eq. (23) but durations ranging from  $D = 0$  to  $D = D_{max}$  were used.

The observed and estimated mean annual maximum flood,  $\mu(D) = E[Q(D)]$ , versus duration  $D$  is presented for each catchment in Figures 3 to 5 and Tables 2 and 3 give the RMSE between observed and estimated  $\mu(D)$ . One can see that QDF models I and II produce similar results. QDF models III and IV are also very similar to one another but their increased flexibility usually allows a better modeling of the mean annual maximum flood for all durations compared to models I and II. In particular, when the instantaneous flood series are not included in the calibration of the models, the QDF models III and IV are usually better than models I and II to estimate the mean instantaneous flood because they reproduce the observed decay of  $\mu(D)$  with  $D$  better. QDF models I and II are unable to model  $\mu(D)$  for VHM-10, VHM-92, VHM-38, and VHM-198 satisfactorily. Results also indicate that QDF models I and II calibrated without instantaneous



values systematically underestimate the mean annual maximum instantaneous flood,  $\mu(D = 0)$ . On the other hand, it appears that  $\mu(D = 0)$  is sometimes overestimated with QDF models III and IV calibrated with  $D \geq 24$ h. Increasing the lower limit for  $\Theta$  (perhaps  $\Theta \geq 0.4$  or  $0.5$ ) could be necessary in order to avoid this overestimation related to very sharp increase of  $\mu(D)$  for low  $D$ .

Outliers in the data set can also account for some of the discrepancies between modeled and observed mean annual maximum flood, in relation for instance to the uncertainty in the rating curve used to convert extreme water-levels into extreme discharge. Also, if the annual maximum flood samples contain floods with different generating mechanisms, or if the flood-generating mechanisms of the annual maximum floods vary with duration  $D$ , then the use of a mixed flood population may introduce uncertainty in the assumptions behind the methodology and the resulting relationships between flood statistics and duration. The observed optimum  $\Delta$  in particular may result from a compromise between different flood types and may not be representative of any specific flood type. Javelle *et al.* (2003) addressed this problem by focusing on spring floods only, which was not done in this study since we are mainly interested in the annual maximum flood.

Appendix I presents the estimated distributions of annual maximum instantaneous flood,  $Q(D = 0)$ , derived with QDF model I (Eq. 3) and QDF model III (Eq. 18), calibrated with and without the use of annual maximum instantaneous floods. The dispersion of the estimated distributions is usually low, indicating that the model assumptions are reasonable.

Appendix II presents the dimensionless parent distributions,  $q(T)$ , estimated with QDF models II and IV calibrated with and without the use of annual maximum instantaneous floods. Here too, the dispersion of the parent distribution is low, indicating that the model assumption regarding invariance of the normalized distributions is reasonable.

In order to compare the skill of the different QDF models with and without inclusion of instantaneous values in their calibration, Figures 6 to 8 present the observed and estimated distributions of annual maximum instantaneous flood,  $Q(D = 0)$ , for each river basin and Tables 4 and 5 give the RMSE between observed and estimated quantiles,  $Q(D = 0, T)$ , for return periods  $T=1.01, 2, 5, 10, 20, 50$  and  $100$  years. The "observed" quantiles were estimated by fitting directly the GEV/PWM distribution to the observed annual maximum instantaneous floods. The results confirm what was already observed with the mean annual maximum flood (see Fig. 3 to 5 and Tables 2 and 3): QDF models III and IV often capture the distribution of instantaneous flood better than QDF models I and II when the instantaneous values are not used in the model calibration but some tendency to overestimate  $Q(D = 0, T)$  is observed when the optimum  $\Theta$  is very low ( $\sim 0.3$ ) and some limitation in the lower limit of this parameter should be considered (perhaps  $\Theta \geq 0.4$  or  $0.5$ ). When instantaneous values are used in the model calibration, all models improve, as expected. Except for a few cases, the estimated distributions of annual maximum instantaneous floods made with the different QDF models are within the 95% confidence interval of the observed distribution.

Finally, Figure 9 presents an example of observed and estimated annual maximum flood distributions,  $Q(D, T)$ , for all durations  $D \geq 24$ h and Figure 10 presents the observed and calculated QDF curves,  $Q(D, T)$ , as a function of duration,  $D$ , for all durations  $D \geq 0$  and return periods  $5 < T \leq 100$  years, for basin VHM-45.

Gauging station	QDF model I ( $D \geq 24h$ )	QDF model I ( $D \geq 0$ )	QDF model III ( $D \geq 24h$ )	QDF model III ( $D \geq 0$ )
VHM-10	5.3	3.3	1.7	0.7
VHM-51	1.2	1.0	0.89	0.58
VHM-92	0.99	0.76	1.03	1.11
VHM-200	10	5.2	5.5	7
VHM-45	1.03	0.87	1.34	0.44
VHM-12	1.07	1.51	1.07	1.51
VHM-19	0.88	0.5	2.4	0.25
VHM-38	0.82	0.79	0.82	0.13
VHM-198	9.98	7.9	18.7	2
VHM-204	1.36	0.98	1.36	0.9

Table 2. RMSE between observed and estimated  $\mu(D)$  using QDF models I and III.

Gauging station	QDF model II ( $D \geq 24h$ )	QDF model II ( $D \geq 0$ )	QDF model IV ( $D \geq 24h$ )	QDF model IV ( $D \geq 0$ )
VHM-10	5.2	3.2	2	0.27
VHM-51	1.12	0.93	1	0.5
VHM-92	1	0.78	0.99	0.09
VHM-200	5.9	4.7	2.5	1.6
VHM-45	1.15	0.92	0.71	0.42
VHM-12	1.37	0.79	1.37	0.79
VHM-19	0.83	0.49	0.65	0.21
VHM-38	0.82	0.80	0.35	0.07
VHM-198	10	8.1	6.16	1.8
VHM-204	0.58	0.48	0.58	0.43

Table 3. RMSE between observed and estimated  $\mu(D)$  using QDF models II and IV.

Gauging station	QDF model I ( $D \geq 24h$ )	QDF model I ( $D \geq 0$ )	QDF model III ( $D \geq 24h$ )	QDF model III ( $D \geq 0$ )
VHM-10	35.4	23.7	12.6	16.8
VHM-51	2.8	3	4.32	1.4
VHM-92	6.15	4.6	3.3	2.2
VHM-200	32.3	15.2	19.8	66.5
VHM-45	10.8	9.1	5.8	6.8
VHM-12	22.6	21.2	22.6	21.2
VHM-19	4.5	2.8	7.8	1.8
VHM-38	11.8	10.9	6.3	8.6
VHM-198	76.4	63.2	60.3	39.3
VHM-204	10.4	7.8	10.4	6.7

Table 4. RMSE between observed and estimated annual maximum instantaneous flood quantiles,  $Q(D = 0, T)$ , using QDF models I and III.

Gauging station	QDF model II ( $D \geq 24h$ )	QDF model II ( $D \geq 0$ )	QDF model IV ( $D \geq 24h$ )	QDF model IV ( $D \geq 0$ )
VHM-10	35.2	25.7	12	16.9
VHM-51	9.	8	4	5.9
VHM-92	6.2	4.9	3.1	2.2
VHM-200	19	18	23.8	33
VHM-45	11.2	10.1	6.4	7.7
VHM-12	17.1	19.9	17.1	19.9
VHM-19	4.4	3.	2.0	2.1
VHM-38	11.8	11.5	7.6	8.7
VHM-198	77	67	25.8	40
VHM-204	11.2	10.4	11.2	9.9

Table 5. RMSE between observed and estimated annual maximum instantaneous flood quantiles,  $Q(D = 0, T)$ , using QDF models II and IV.

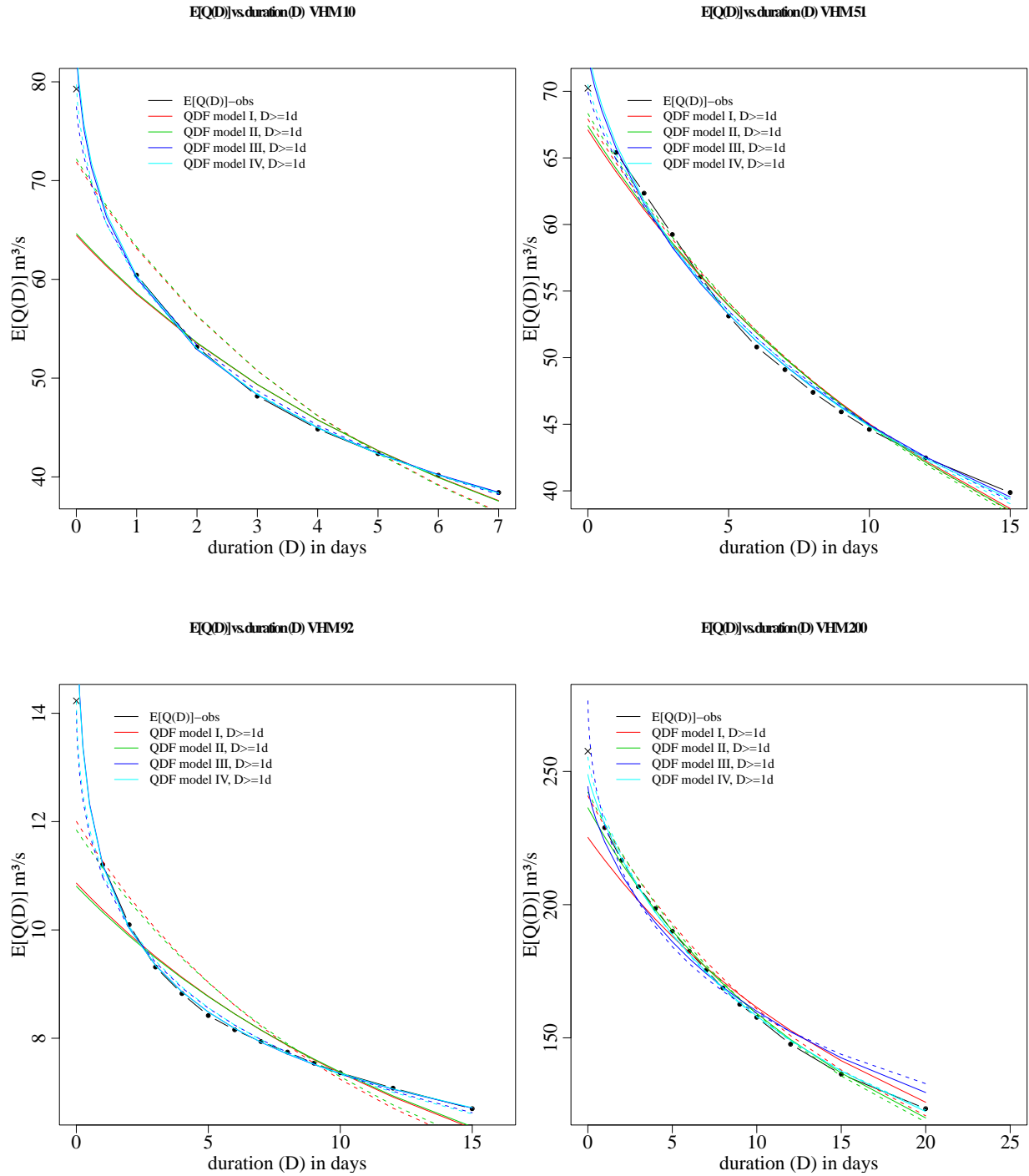


Figure 3. Observed and estimated mean annual maximum flood,  $\mu(D)$  vs. duration  $D$ , at VHM-10 (top-left), VHM-51 (top-right), VHM-92 (bottom-left) and VHM-200 (bottom-right). The black symbols and solid black line correspond to the observations. The solid colored lines correspond to QDF models I to IV calibrated without instantaneous values ( $D \geq 24\text{h}$ ). The dashed colored lines correspond to QDF models I to IV calibrated with instantaneous values ( $D \geq 0$ ).

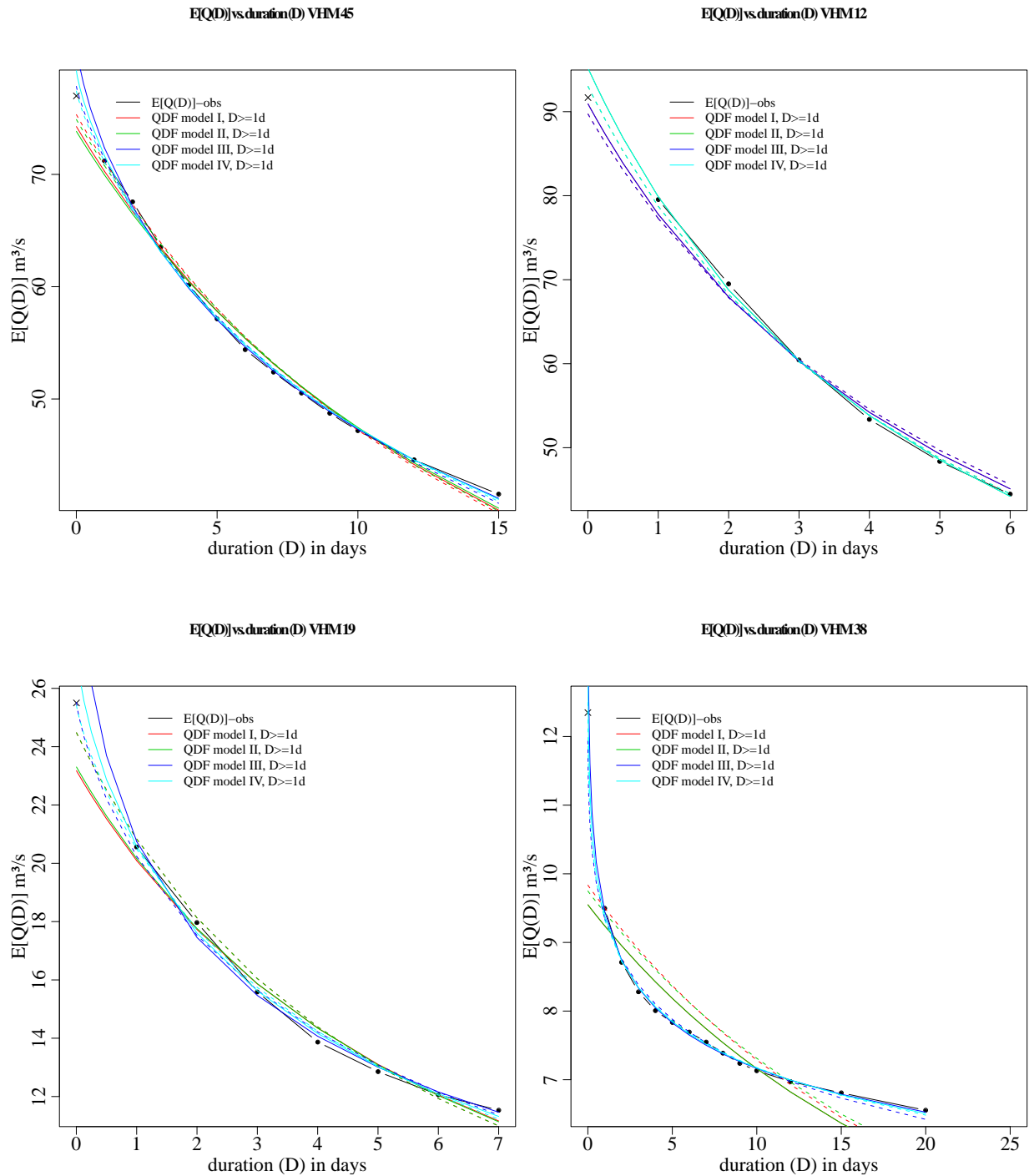
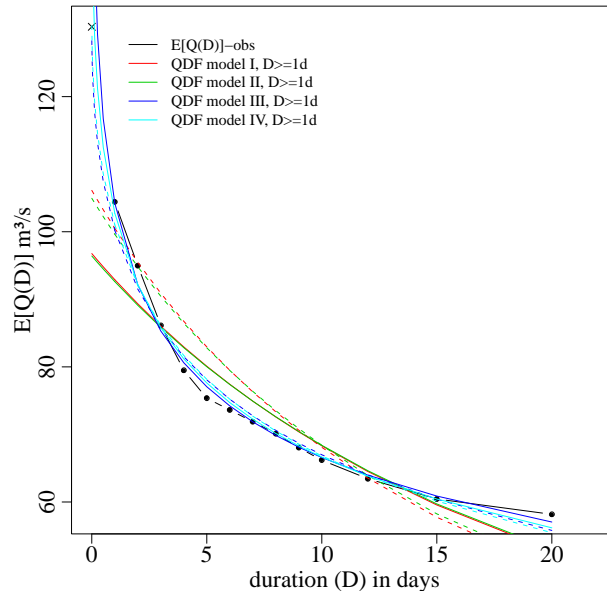


Figure 4. Observed and estimated mean annual maximum flood,  $\mu(D)$  vs. duration  $D$ , at VHM-45 (top-left), VHM-12 (top-right), VHM-19 (bottom-left) and VHM-38 (bottom-right). See caption of Fig. 3.

**E[Q(D)] vs duration(D) VHM198**



**E[Q(D)] vs duration(D) VHM204**

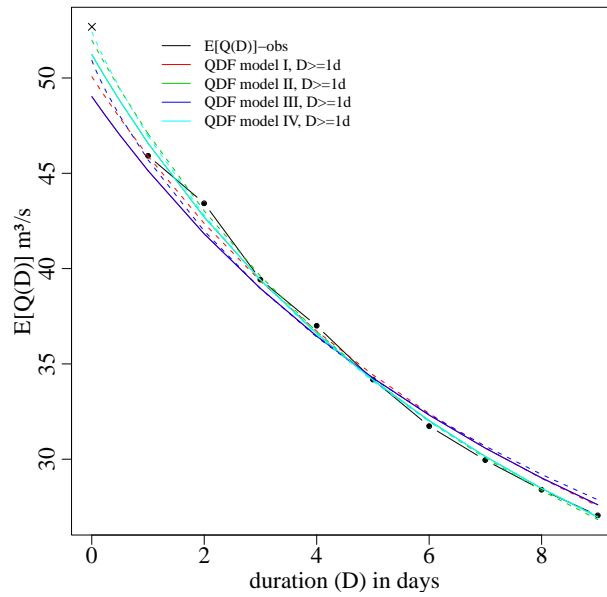


Figure 5. Observed and estimated mean annual maximum flood,  $\mu(D)$  vs. duration  $D$ , at VHM-198 (top) and VHM-204 (bottom). See caption of Fig. 3.

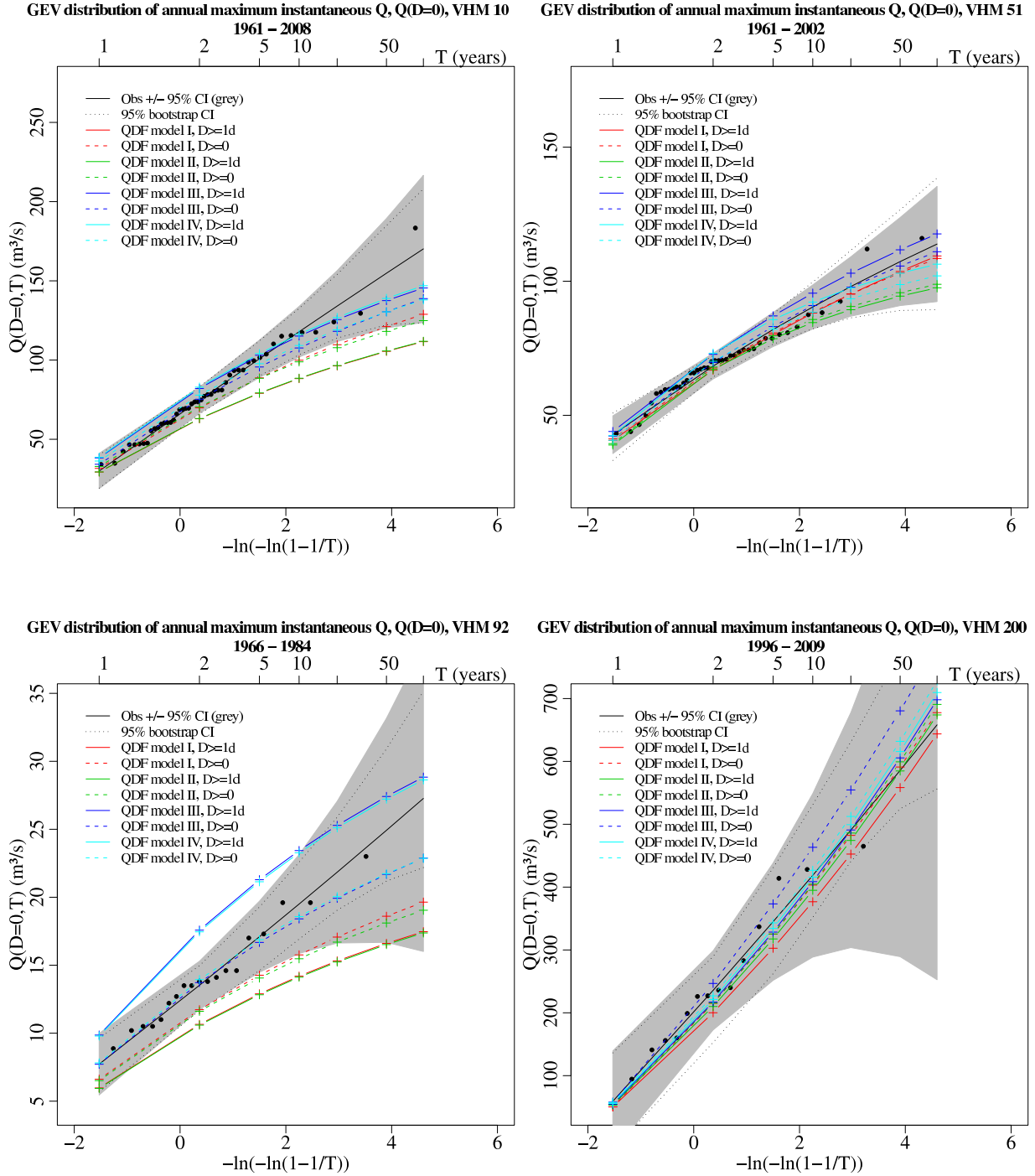


Figure 6. Observed and estimated cumulative distribution functions for annual maximum instantaneous flood,  $Q(D = 0)$ , at VHM-10 (top-left), VHM-51 (top-right), VHM-92 (bottom-left) and VHM-200 (bottom-right). The solid black line represents the reference GEV/PWM distribution estimated on the observed instantaneous flood sample (black symbols), the grey shaded region represents the 95% confidence interval and the dotted black line the 95% bootstrap confidence interval. The solid colored lines correspond to the GEV distributions estimated with QDF models I to IV (Eqs. (3), (11), (18) and (21)) calibrated without using the instantaneous values ( $D \geq 24h$ ) and the dashed colored lines correspond to the GEV distributions estimated with QDF models I to IV calibrated with instantaneous values ( $D \geq 0$ ).

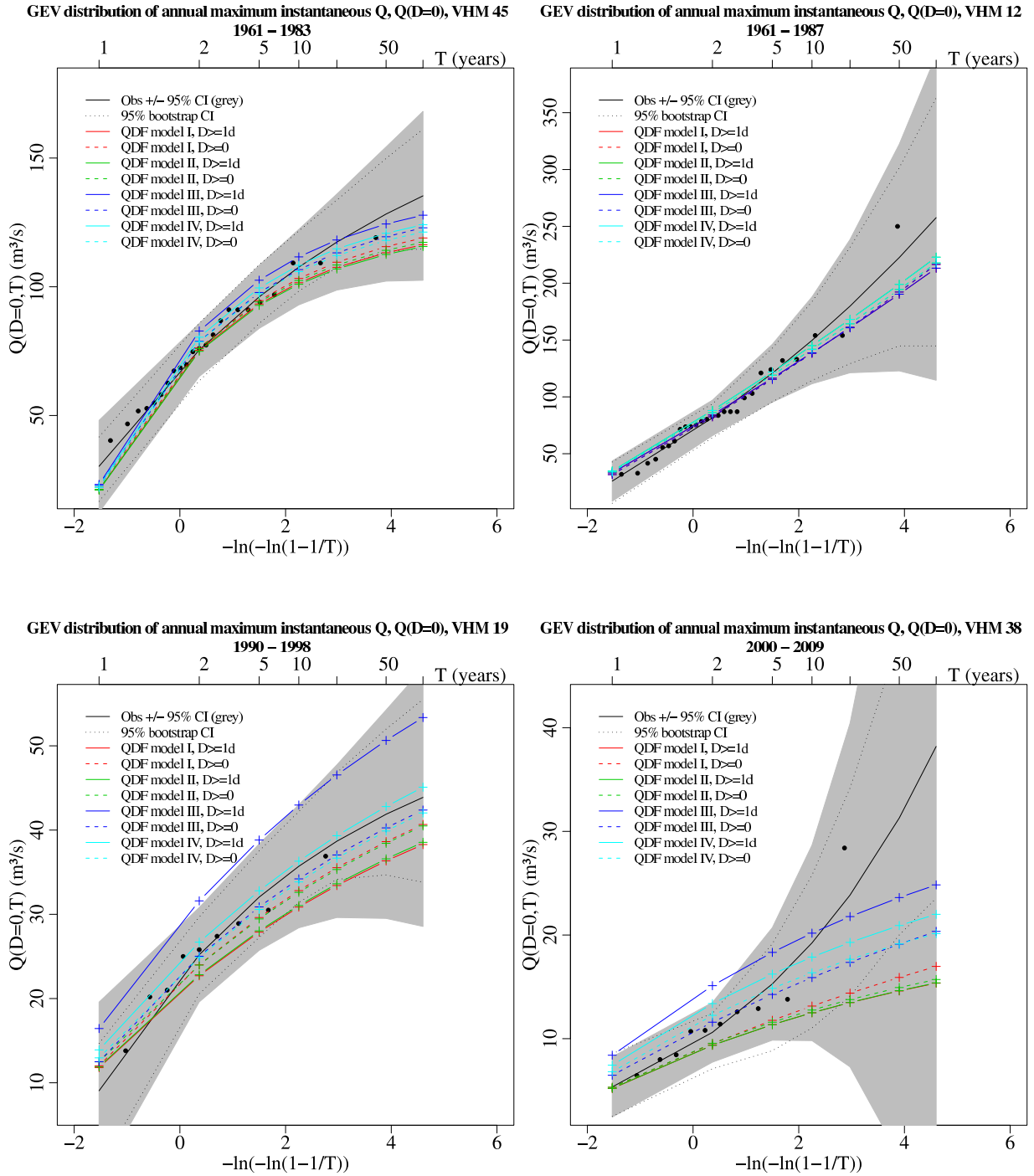


Figure 7. Observed and estimated cumulative distribution functions for annual maximum instantaneous flood,  $Q(D = 0)$ , at VHM-45 (top-left), VHM-12 (top-right), VHM-19 (bottom-left) and VHM-38 (bottom-right). See caption of Fig. 6.



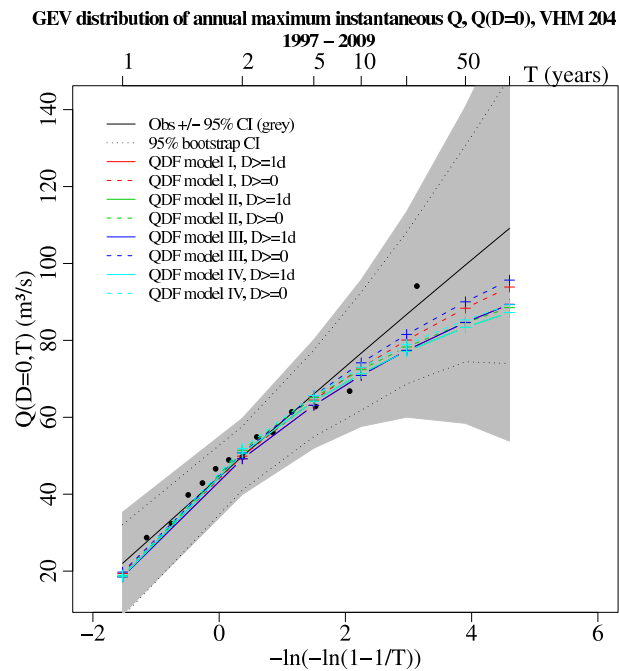
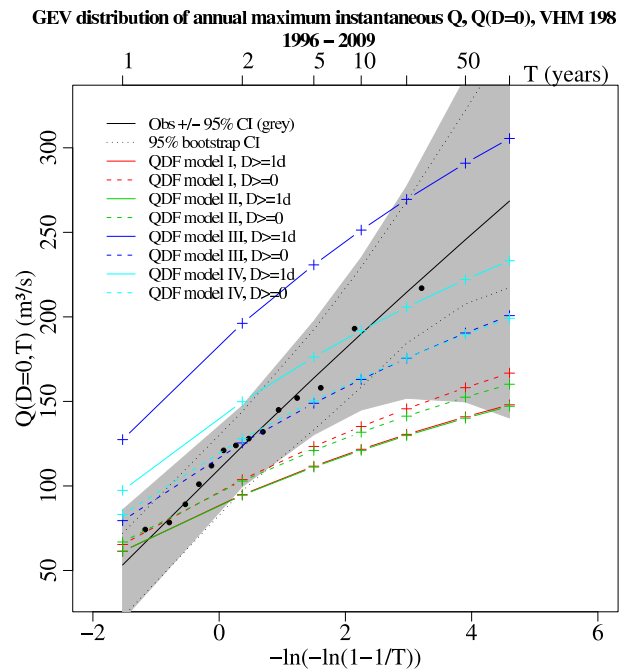


Figure 8. Observed and estimated cumulative distribution functions for annual maximum instantaneous flood,  $Q(D = 0)$ , at VHM-198 (top) and VHM-204 (bottom). See caption of fig. 6.

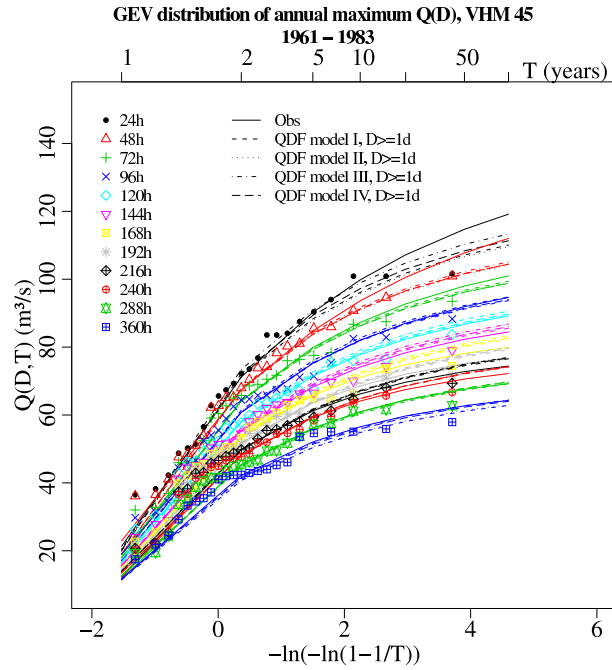


Figure 9. Example of observed and estimated cumulative distribution functions of annual maximum flood of duration  $D$ ,  $Q(D)$ , at VHM-45. The solid lines represents the reference GEV/PWM distribution estimated on the observed flood samples (symbols). The dashed lines correspond to the GEV distributions estimated with the QDF models I to IV calibrated without using the instantaneous values ( $D \geq 24h$ ).

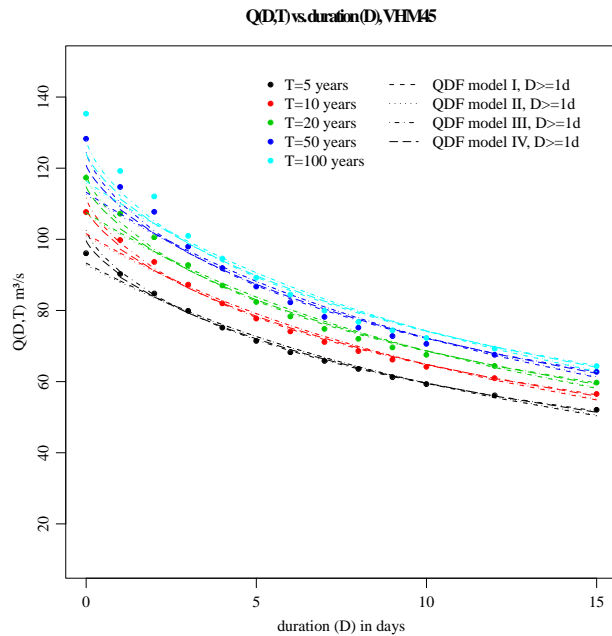


Figure 10. Example of observed and estimated QDF curves,  $Q(D,T)$ , at VHM-45 for  $T=5, 10, 20, 50$  and  $100$  years. The symbols corresponds to the reference QDF curves calculated from the GEV distributions directly adjusted on the observed flood samples for the duration  $D$  and the lines the QDF curves estimated from QDF models I to IV and calibrated without using the instantaneous values ( $D \geq 24h$ ).

## 5 Conclusion and future research

A methodology for modeling QDF curves based on the so-called continuous converging model has been applied to ten river basins in Northern Iceland. Several models were tested and the model assumptions were found to be valid in most cases. The QDF models allow the calculation of extreme flood quantiles as a continuous function of duration and return period with a single and straightforward formula. These QDF curves give a complete description of the flood dynamics of a basin which is very useful in flood studies. This methodology looks promising and should be extended to other river basins in Iceland. QDF modeling is potentially useful for deriving extreme flood statistics of any duration  $D$  and in particular instantaneous flood ( $D=0$ ) from daily discharge series simulated with the WaSiM-ETH distributed hydrological model used at IMO and will enhance its application. Several applications of this methodology will be investigated in the future such as separately analysing the floods according to their generating mechanisms. The development of a regional QDF modeling by merging the local QDF analysis presented in this study with the regional flood frequency analysis presented in Crochet (2012) also looks promising and will be investigated.

## 6 Acknowledgements

This study was supported by Vegagerðin (the Icelandic Road Administration). The author gratefully acknowledges Auður Atladóttir, Davíð Egilsson and Gunnar Sigurðsson for their assistance in providing streamflow data and Tinna Þórarinsdóttir for interesting discussions during the development of this work.

## 7 References

- Atladóttir A., P. Crochet, S. Jónsson and H.B. Hróðmarsson. 2011. Mat á flóðagreiningu með rennslisröðum reiknuðum með vatnafræðilíkaninu WaSiM. Frumniðurstöður fyrir vatnasvið á sunnanverðum Vestfjörðum. Icelandic Meteorological Office, Rep. 2011-008, 41 pp.
- Crochet, P. 2012. Estimating the flood frequency distribution for ungauged catchments using an index flood procedure. Application to ten catchments in Northern Iceland. Icelandic Meteorological Office, Rep. 2012-005, 59pp.
- Crochet, P., T. Jóhannesson, T. Jónsson, O. Sigurðsson, H. Björnsson, F. Pálsson and I. Barstad. 2007. Estimating the spatial distribution of precipitation in Iceland using a linear model of orographic precipitation. *J. Hydrometeorol.*, 8, 1285–1306.
- Eliasson, J. 2000. Design values for precipitation and floods from M5 values. *Nordic Hydrology*, 31 (4/5), 357–372.
- Hosking, J.R.M, J.R. Wallis, and E.F. Wood. 1985a. Estimation of the generalized extreme-value distribution by the method of the probability-weighted moments. *Technometrics*, 27(3), 251–261.
- Hosking, J.R.M, J.R. Wallis, and E.F. Wood. 1985b. An appraisal of the regional flood frequency procedure in the UK Flood Studies Report. *Hydrol. Sci. J.*, 30, 85–109.
- Javelle, P., T.B.M.J. Ouarda, M. Lang, B. Bobée, G. Galéa and J.M. Grésillon. 2002. Development of regional flood-duration-frequency curves based on the index-flood method. *J. Hydrol.*, 258, 249–259.
- Javelle, P., T.B.M.J. Ouarda and B. Bobée. 2003. Spring flood analysis using the flood-duration-frequency approach: application to the provinces of Quebec and Ontario, Canada. *Hydrol. Proc.*, 17, 3717–3736.

**Appendix-I: Estimated GEV/PWM cumulative distribution functions (CDF) of annual maximum instantaneous flood using QDF models I and III**

**GEV distribution of annual max. instantaneous  $Q$ ,  $Q(D=0)$ ,  
derived from QDF models I and III, for VHM 10**

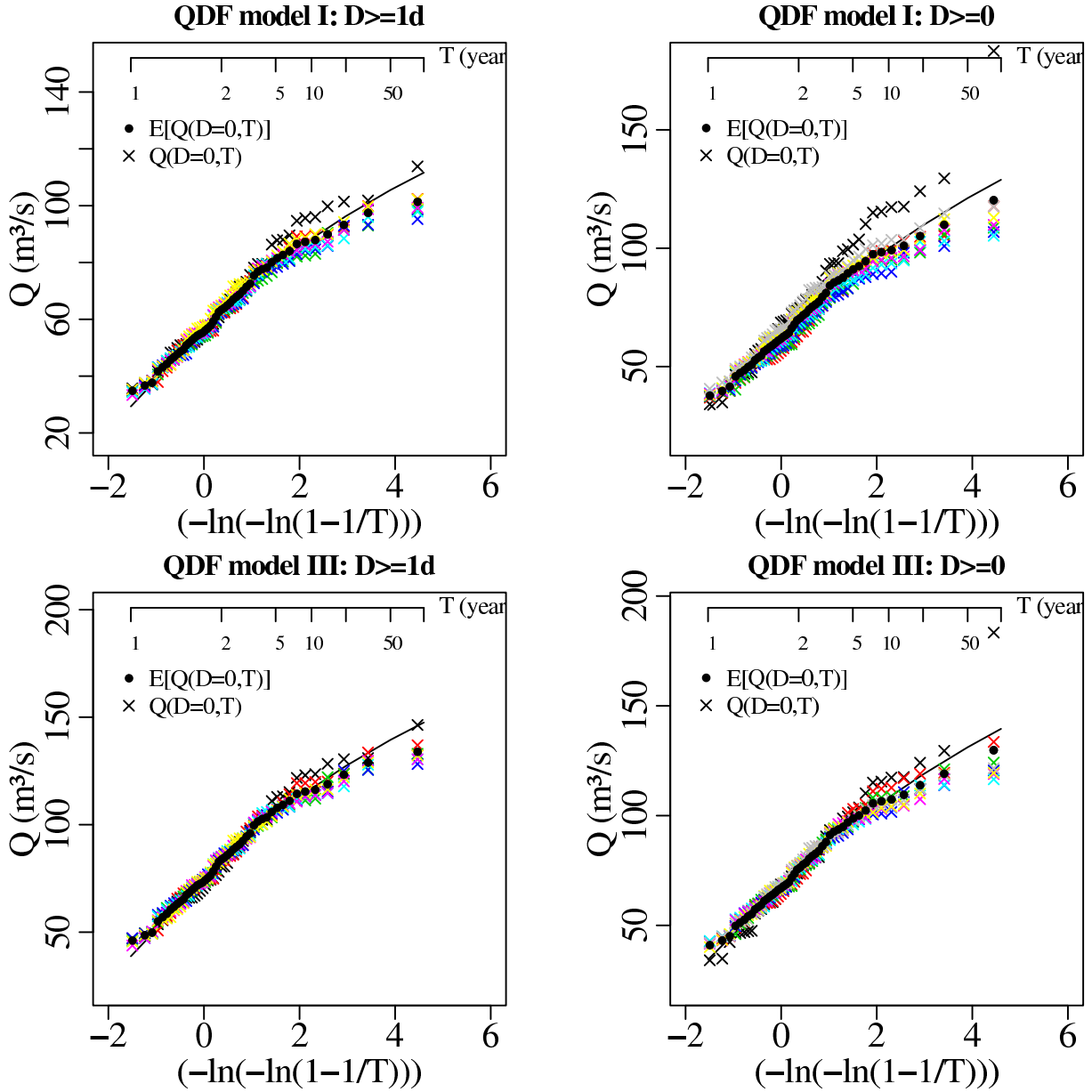


*Figure I.1. Estimated GEV/PWM CDF of annual maximum instantaneous flood,  $Q(D=0)$ , derived from QDF models I and III, for basin VHM-10. This is obtained by scaling the CDF of annual maximum flood of duration  $D$ ,  $Q(D)$ , with QDF models I and III. The solid black line represents the CDF calculated from the average values over all durations (Eq. 7) and each colored symbol corresponds to  $Q(D=0)$  derived from duration  $D$ . Top-left: QDF model I with  $D \geq 24h$ , Top-right: QDF model I with  $D \geq 0$ , Bottom-left: QDF model III with  $D \geq 24h$ , Bottom-right: QDF model III with  $D \geq 0$ .*

**GEV distribution of annual max. instantaneous  $Q$ ,  $Q(D=0)$ ,  
derived from QDF models I and III, for VHM 51**

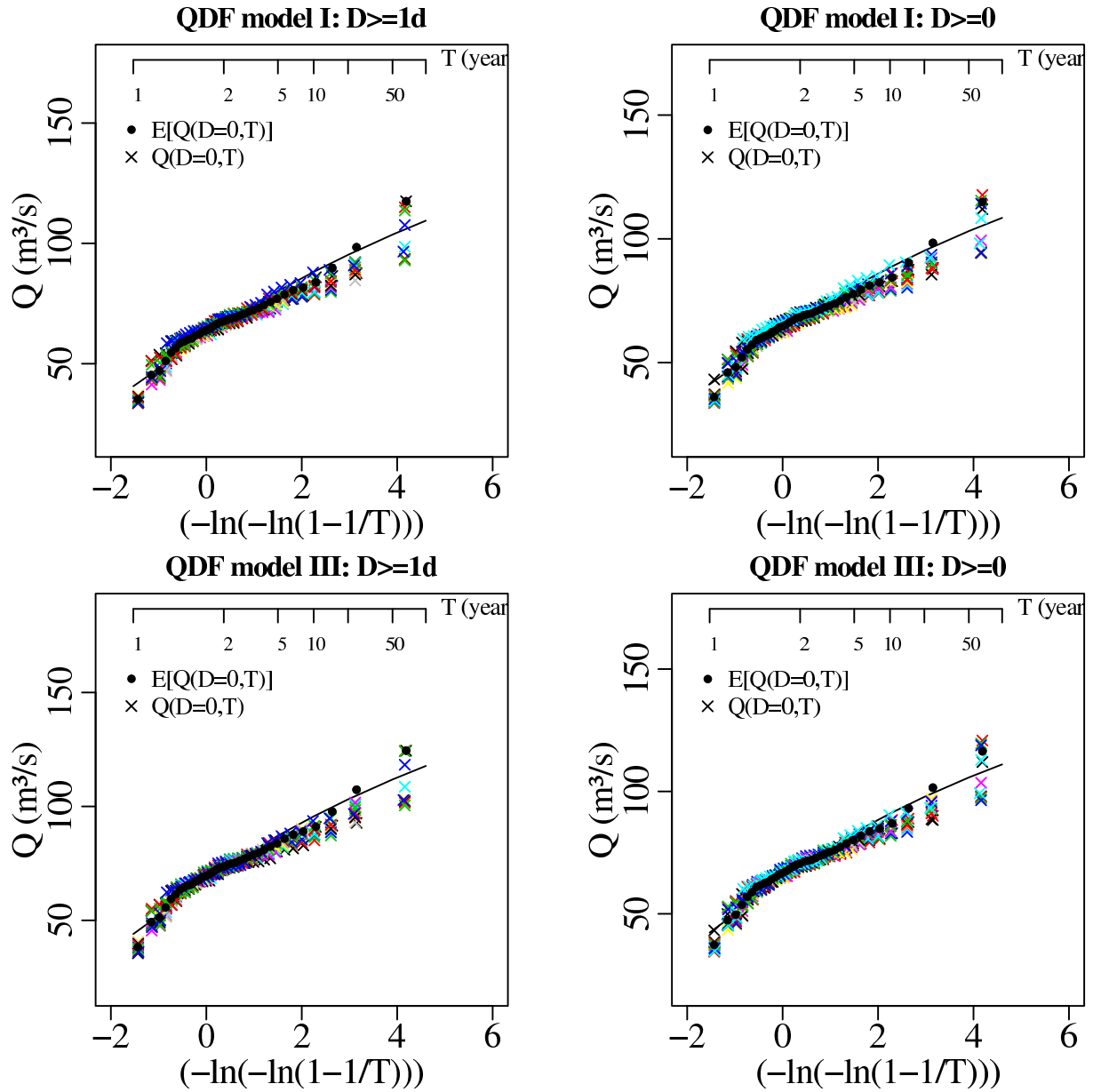


*Figure I.2. Estimated CDF of annual maximum instantaneous flood,  $Q(D = 0)$ , derived from QDF models I and III, for basin VHM-51. See caption of Fig. I.1.*

GEV distribution of annual max. instantaneous  $Q$ ,  $Q(D=0)$ ,  
 derived from QDF models I and III, for VHM 92

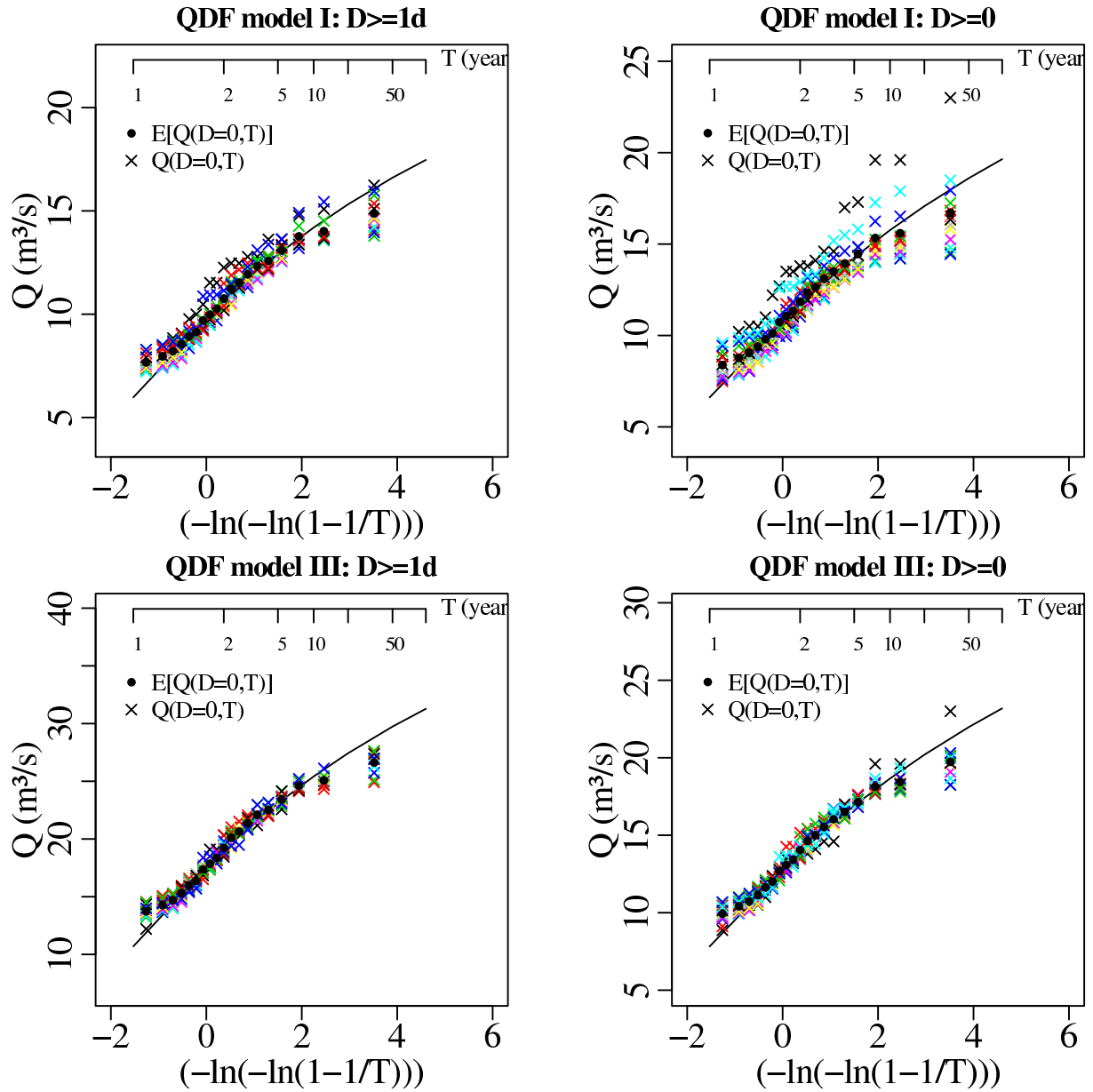
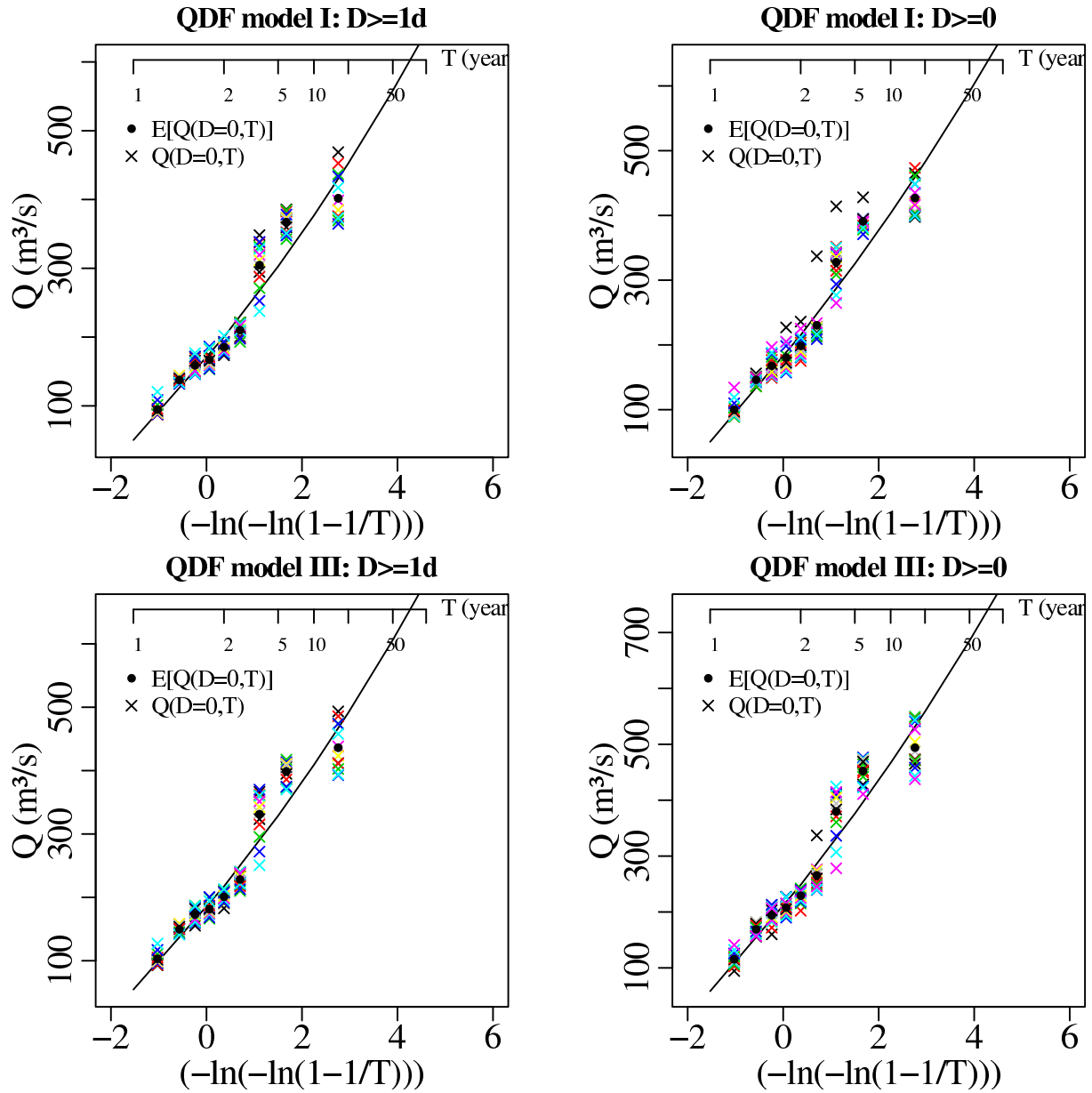


Figure I.3. Estimated CDF of annual maximum instantaneous flood,  $Q(D = 0)$ , derived from QDF models I and III, for basin VHM-92. See caption of Fig. I.1.



**GEV distribution of annual max. instantaneous  $Q$ ,  $Q(D=0)$ ,  
derived from QDF models I and III, for VHM 200**



*Figure I.4. Estimated CDF of annual maximum instantaneous flood,  $Q(D = 0)$ , derived from QDF models I and III, for basin VHM-200. See caption of Fig. I.1.*

GEV distribution of annual max. instantaneous  $Q$ ,  $Q(D=0)$ ,  
 derived from QDF models I and III, for VHM 45

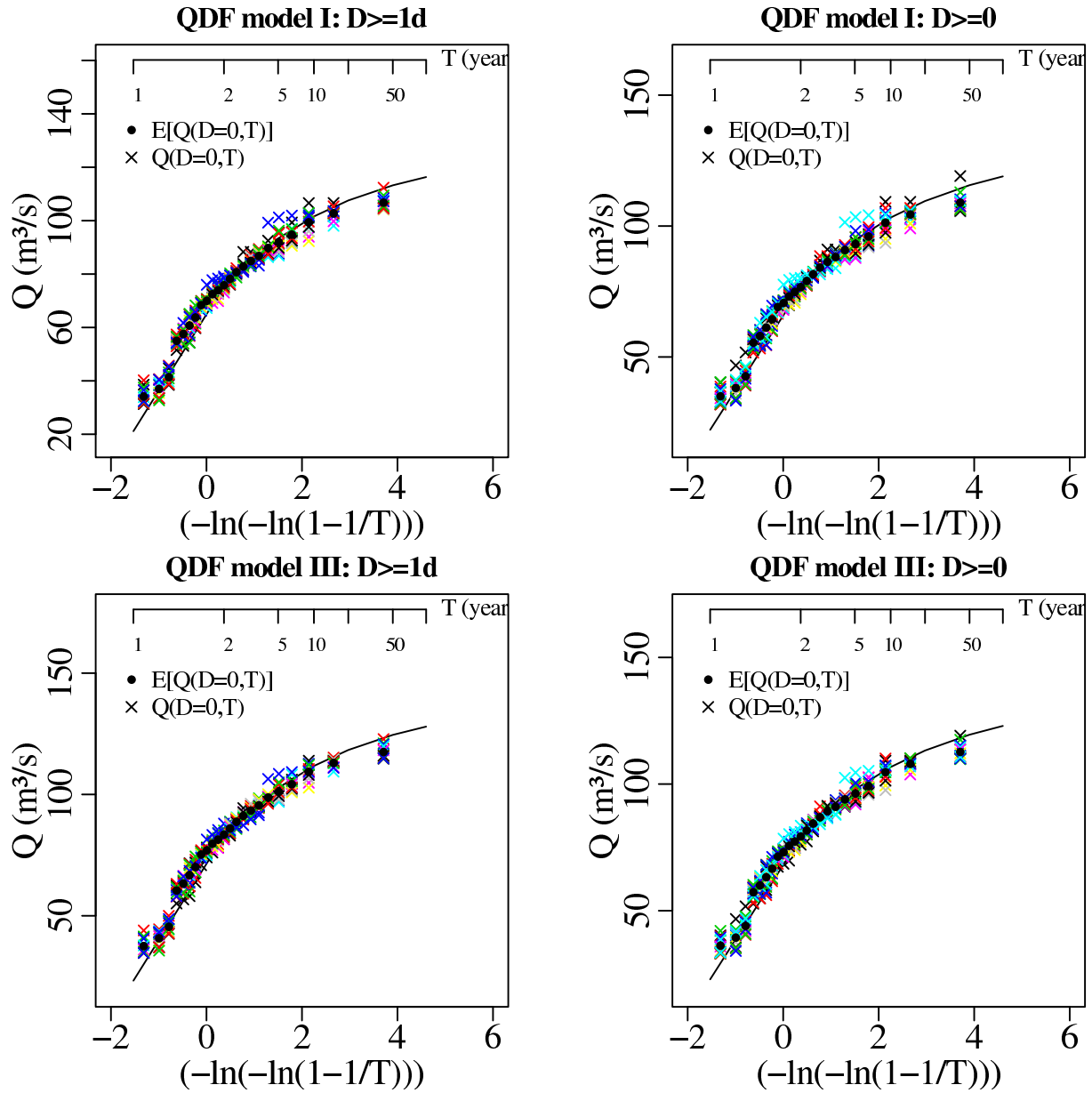


Figure I.5. Estimated CDF of annual maximum instantaneous flood,  $Q(D = 0)$ , derived from QDF models I and III, for basin VHM-45. See caption of Fig. I.1.

GEV distribution of annual max. instantaneous  $Q$ ,  $Q(D=0)$ ,  
 derived from QDF models I and III, for VHM 12

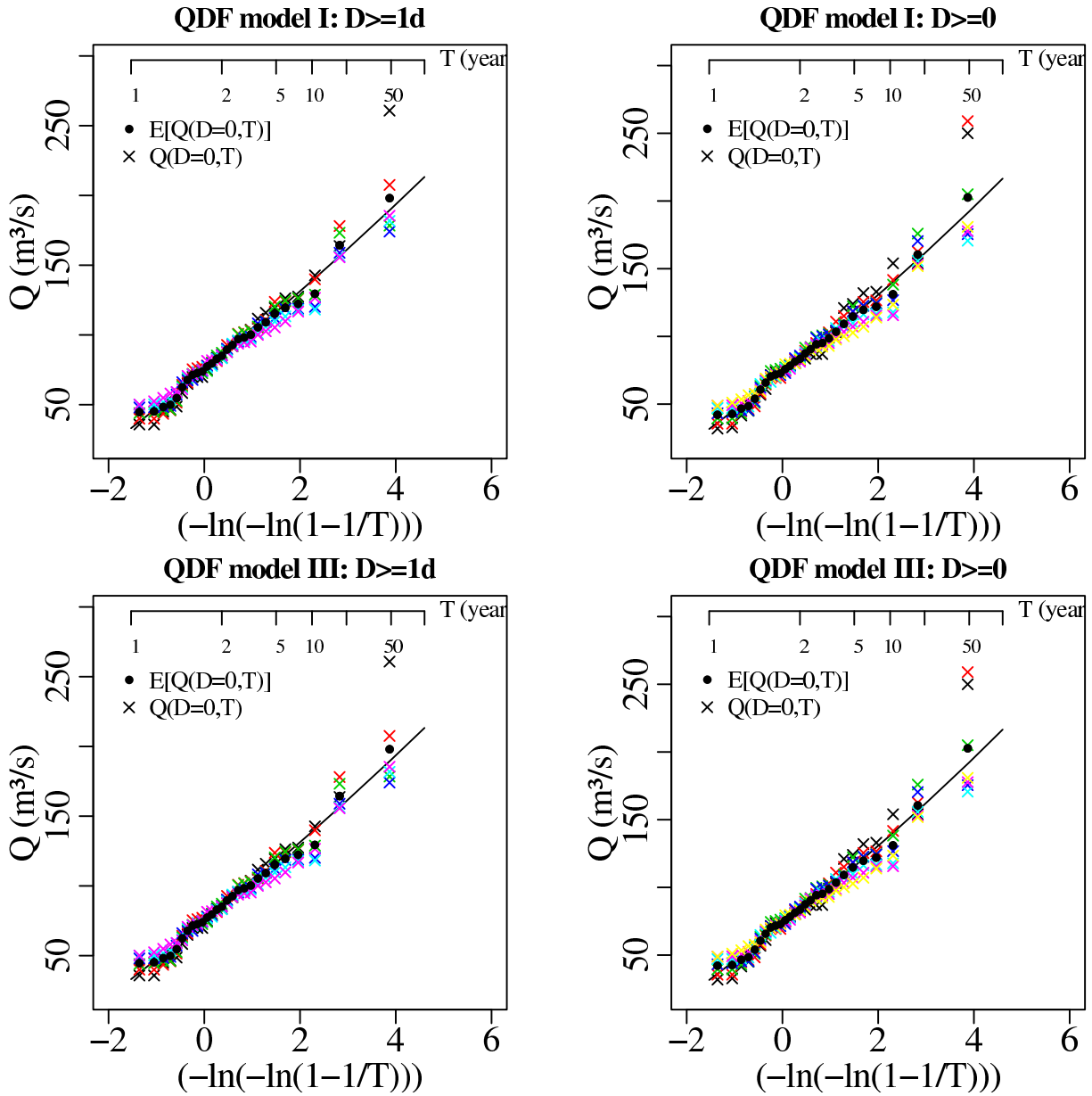
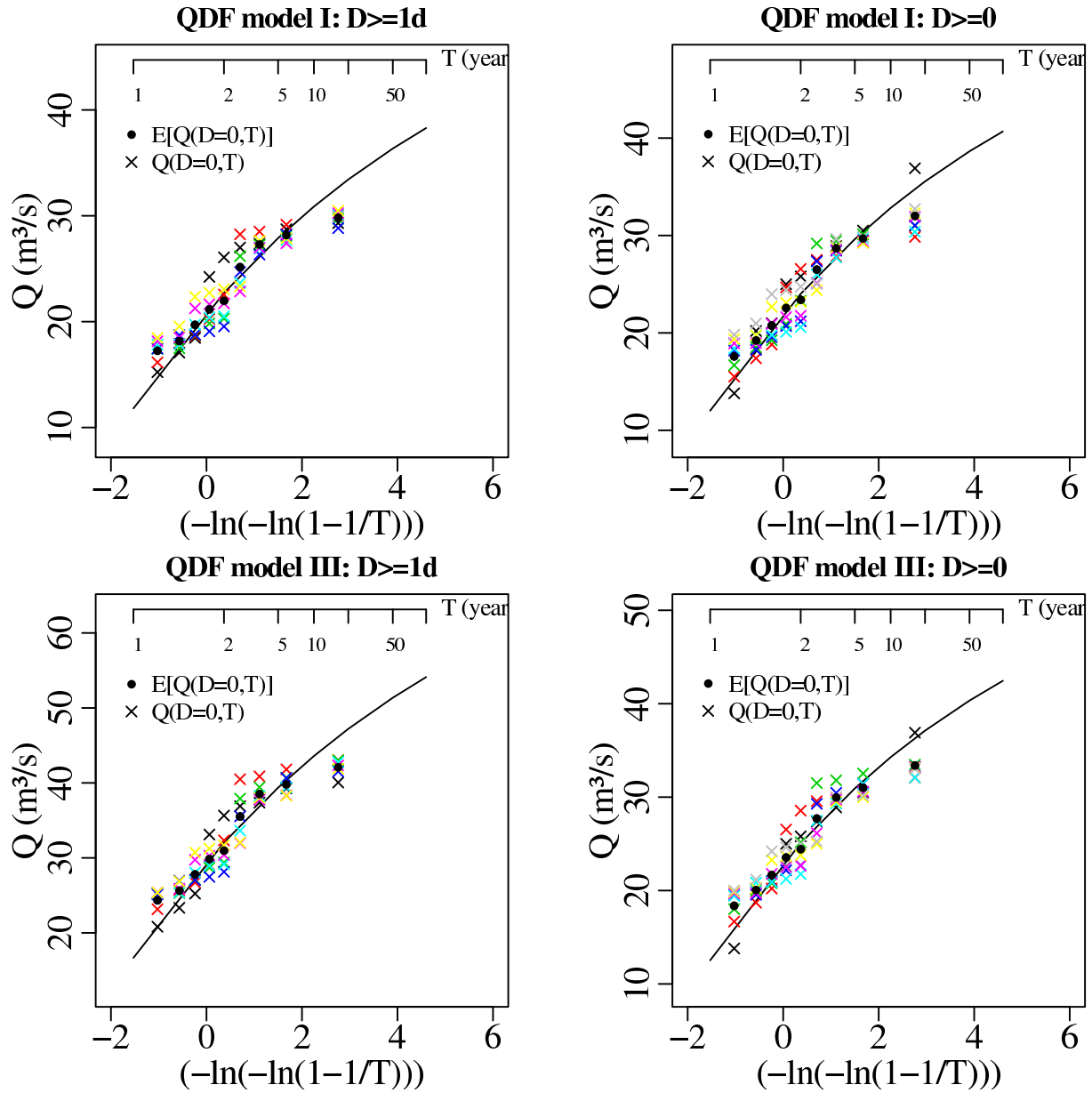


Figure I.6. Estimated CDF of annual maximum instantaneous flood,  $Q(D = 0)$ , derived from QDF models I and III, for basin VHM-12. See caption of Fig. I.1.

**GEV distribution of annual max. instantaneous  $Q$ ,  $Q(D=0)$ ,  
derived from QDF models I and III, for VHM 19**



*Figure I.7. Estimated CDF of annual maximum instantaneous flood,  $Q(D = 0)$ , derived from QDF models I and III, for basin VHM-19. See caption of Fig. I.1.*

GEV distribution of annual max. instantaneous  $Q$ ,  $Q(D=0)$ ,  
 derived from QDF models I and III, for VHM 38

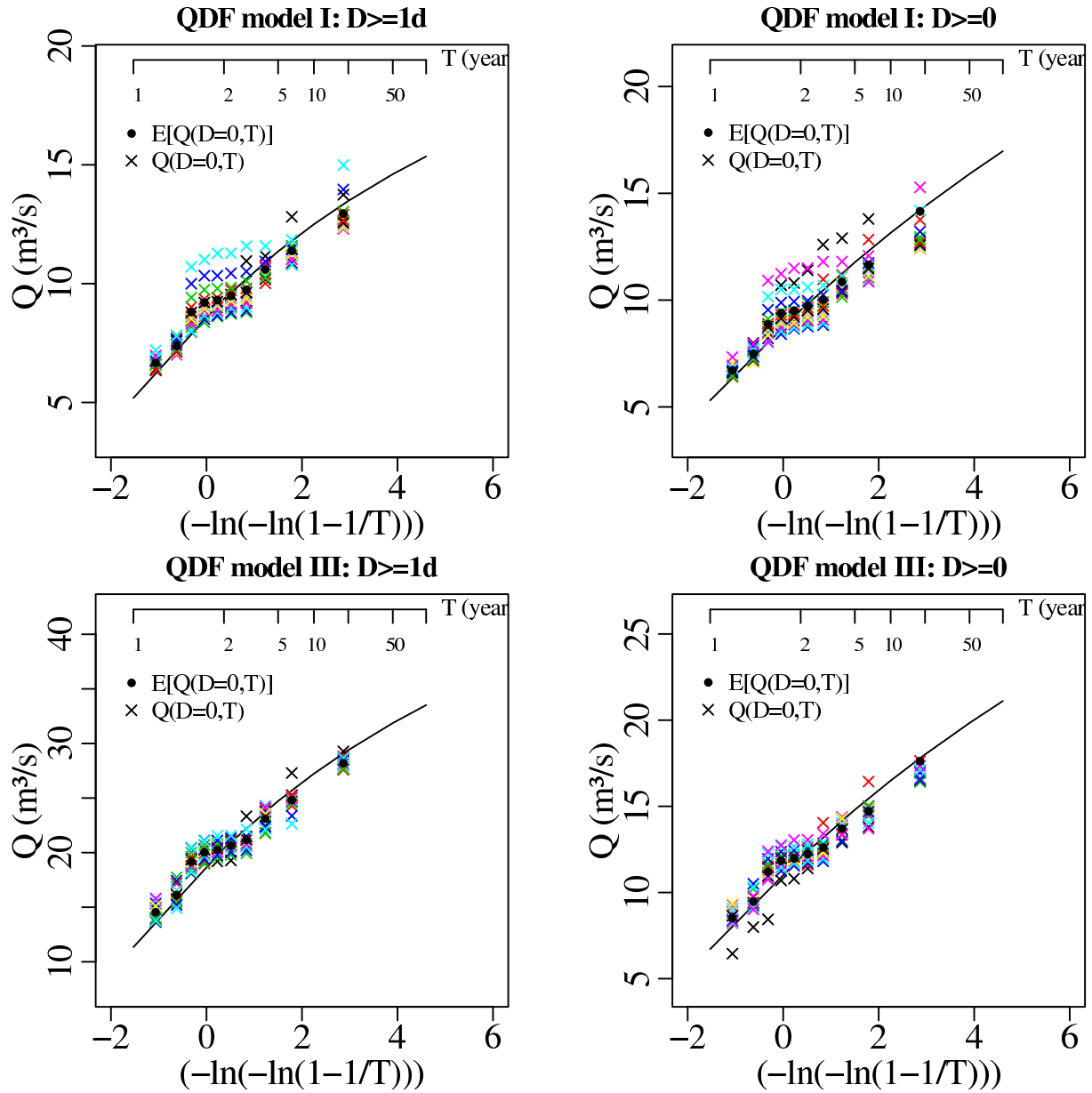


Figure I.8. Estimated CDF of annual maximum instantaneous flood,  $Q(D = 0)$ , derived from QDF models I and III, for basin VHM-38. See caption of Fig. I.1.

GEV distribution of annual max. instantaneous  $Q$ ,  $Q(D=0)$ ,  
 derived from QDF models I and III, for VHM 198

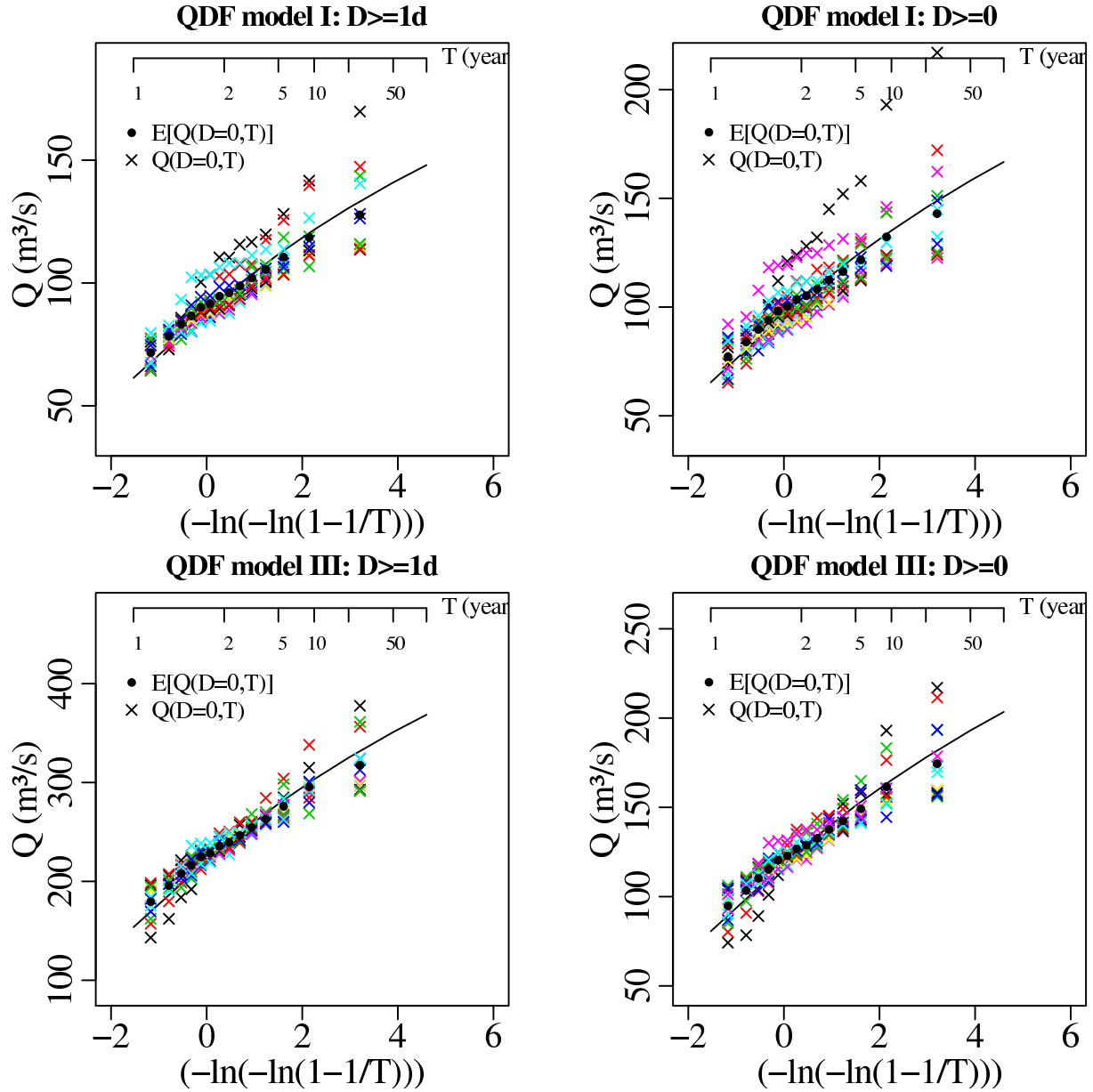


Figure I.9. Estimated CDF of annual maximum instantaneous flood,  $Q(D = 0)$ , derived from QDF models I and III, for basin VHM-198. See caption of Fig. I.1.

GEV distribution of annual max. instantaneous  $Q$ ,  $Q(D=0)$ ,  
 derived from QDF models I and III, for VHM 204

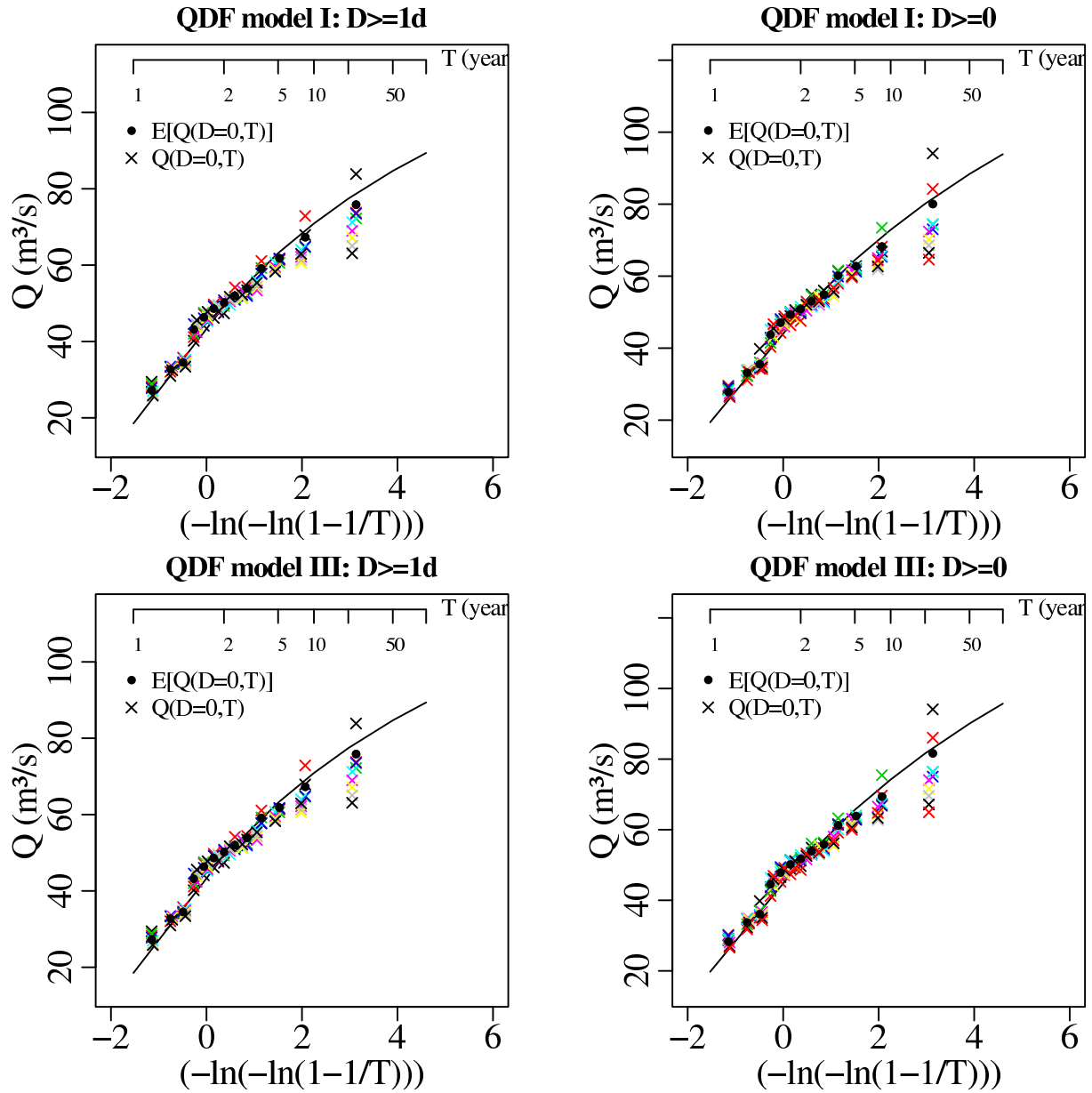
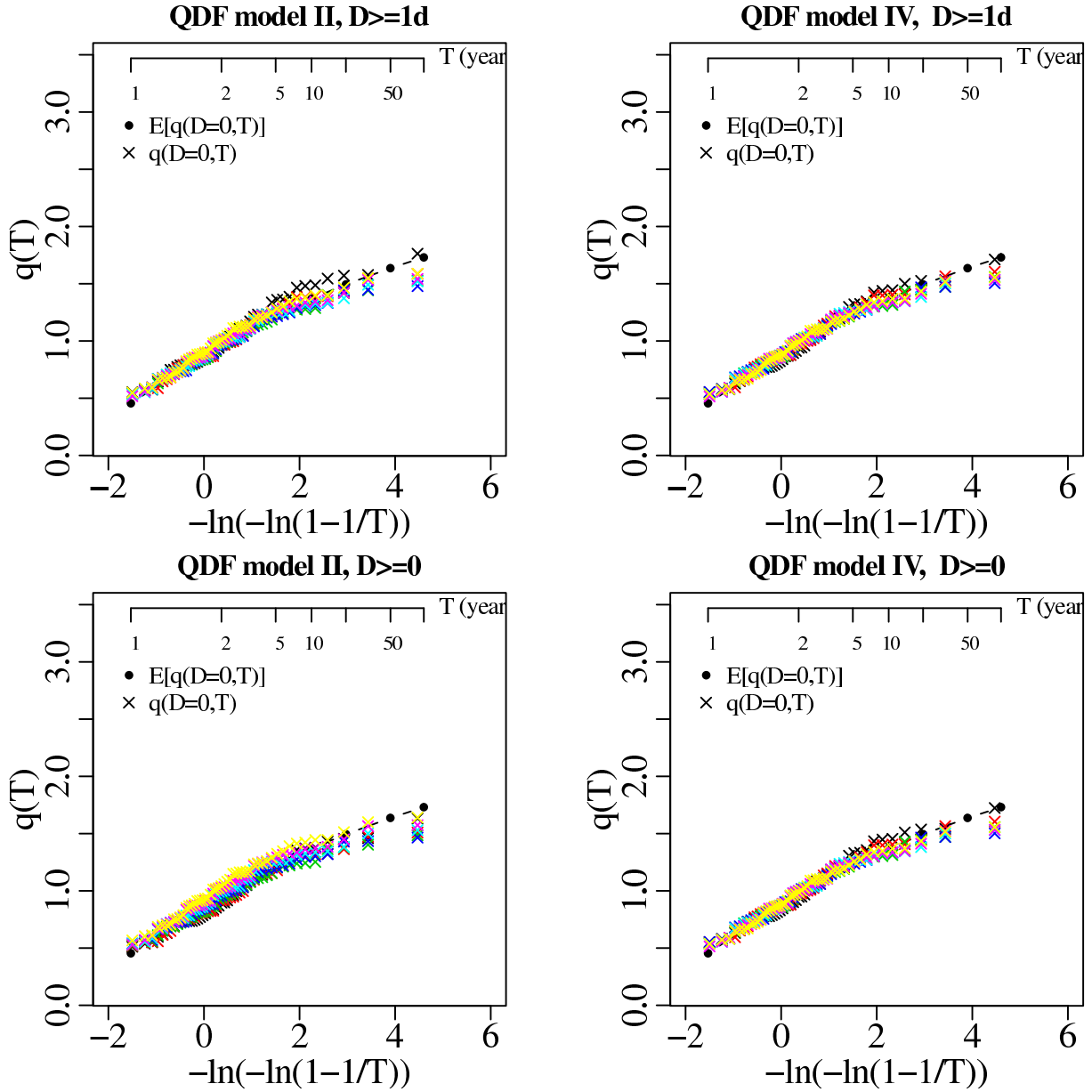


Figure I.10. Estimated CDF of annual maximum instantaneous flood,  $Q(D = 0)$ , derived from QDF models I and III, for basin VHM-204. See caption of Fig. I.1.

**Appendix-II: Estimated dimensionless parent cumulative distribution functions (CDF),  $q(T)$ , using QDF models II and IV**



**Parent distribution  $q(T)$   
VHM 10**



*Figure II.1. Estimated dimensionless parent CDF,  $q(T)$ , for basin VHM-10, using the regional GEV/PWM (black dashed line). The other distributions (coloured symbols) represent the individual parent CDFs derived from each flood sample of duration  $D$ . Top-left: QDF model II with  $D \geq 24h$ , Top-right: QDF model IV with  $D \geq 24h$ , Bottom-left: QDF model II with  $D \geq 0$ , Bottom-right: QDF model IV with  $D \geq 0$ .*

Parent distribution  $q(T)$   
VHM 51

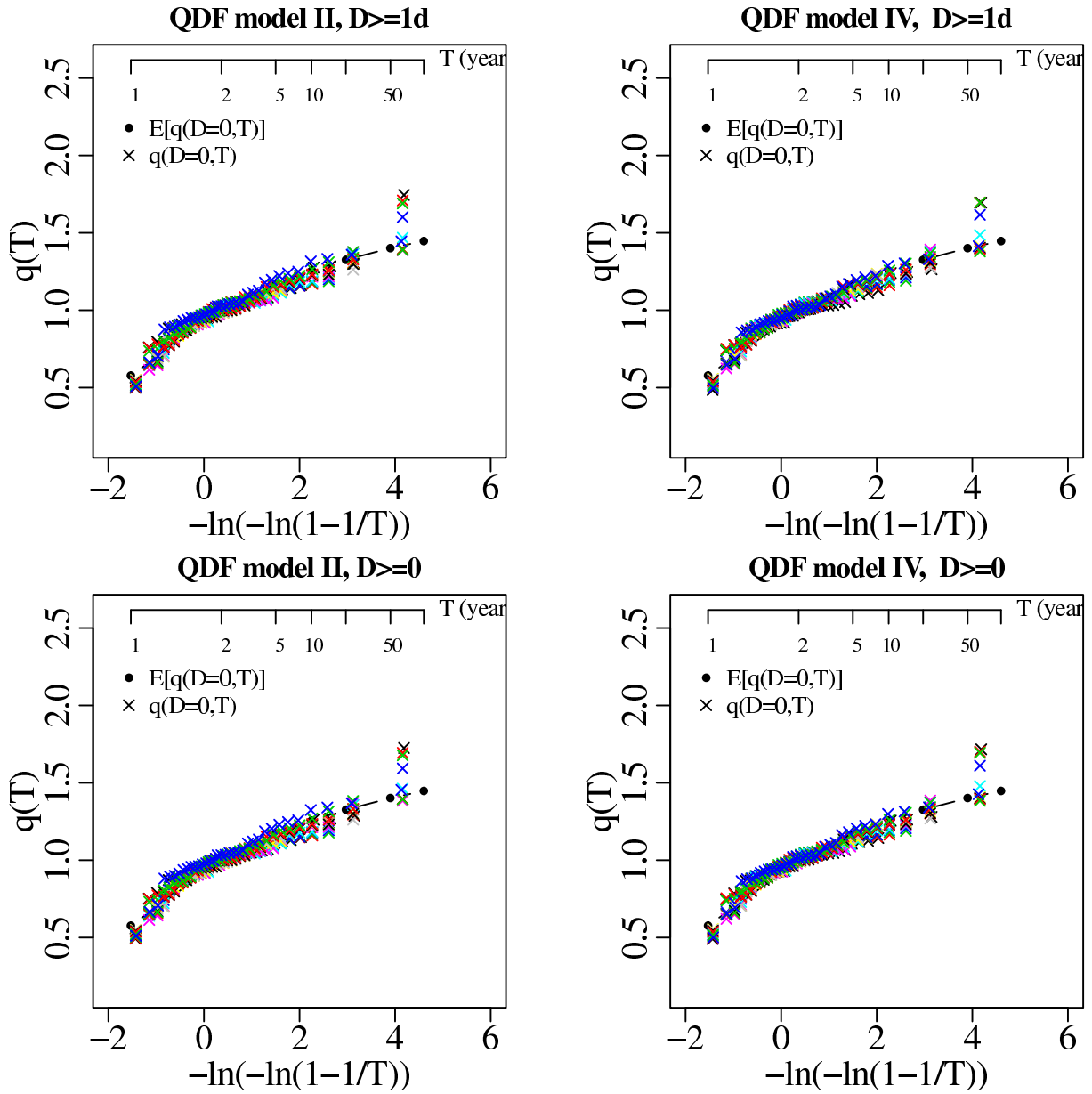


Figure II.2. Estimated dimensionless parent CDF,  $q(T)$ , for basin VHM-51. See caption of fig. II.1.

**Parent distribution  $q(T)$   
VHM 92**

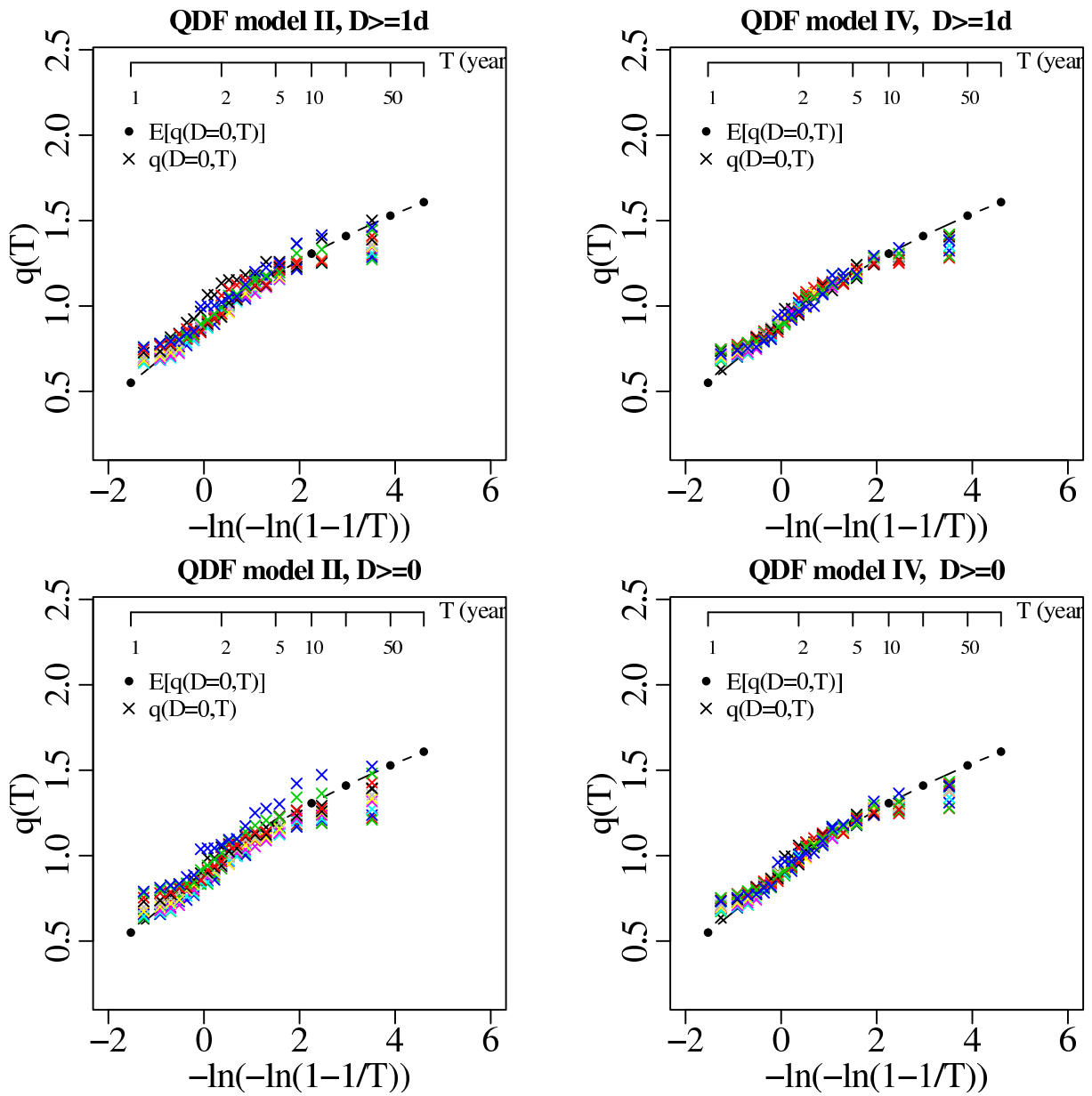


Figure II.3. Estimated dimensionless parent CDF,  $q(T)$ , for basin VHM-92. See caption of fig. II.1.

**Parent distribution  $q(T)$   
VHM 200**

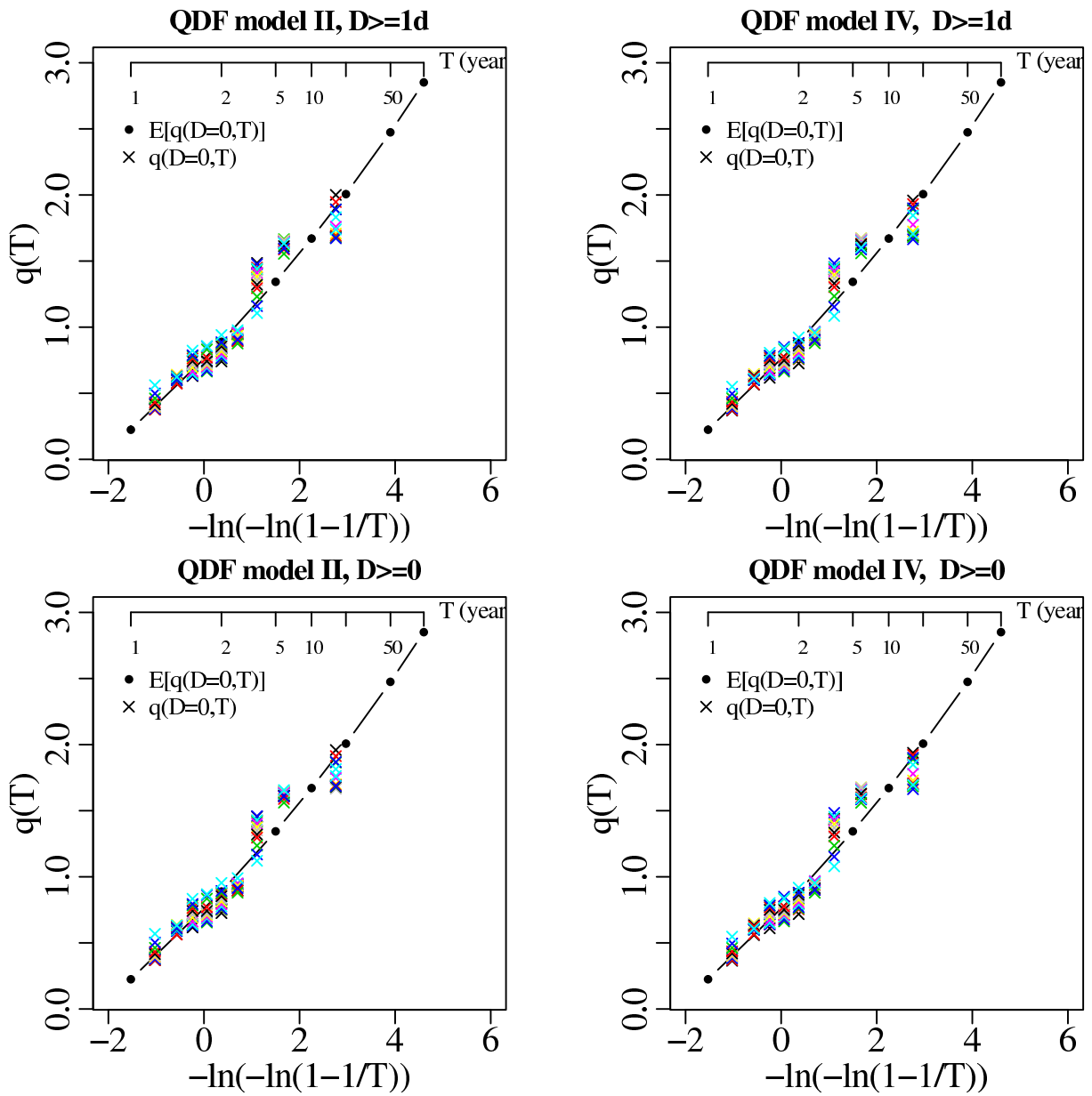


Figure II.4. Estimated dimensionless parent CDF,  $q(T)$ , for basin VHM-200. See caption of fig. II.1.

Parent distribution  $q(T)$   
VHM 45

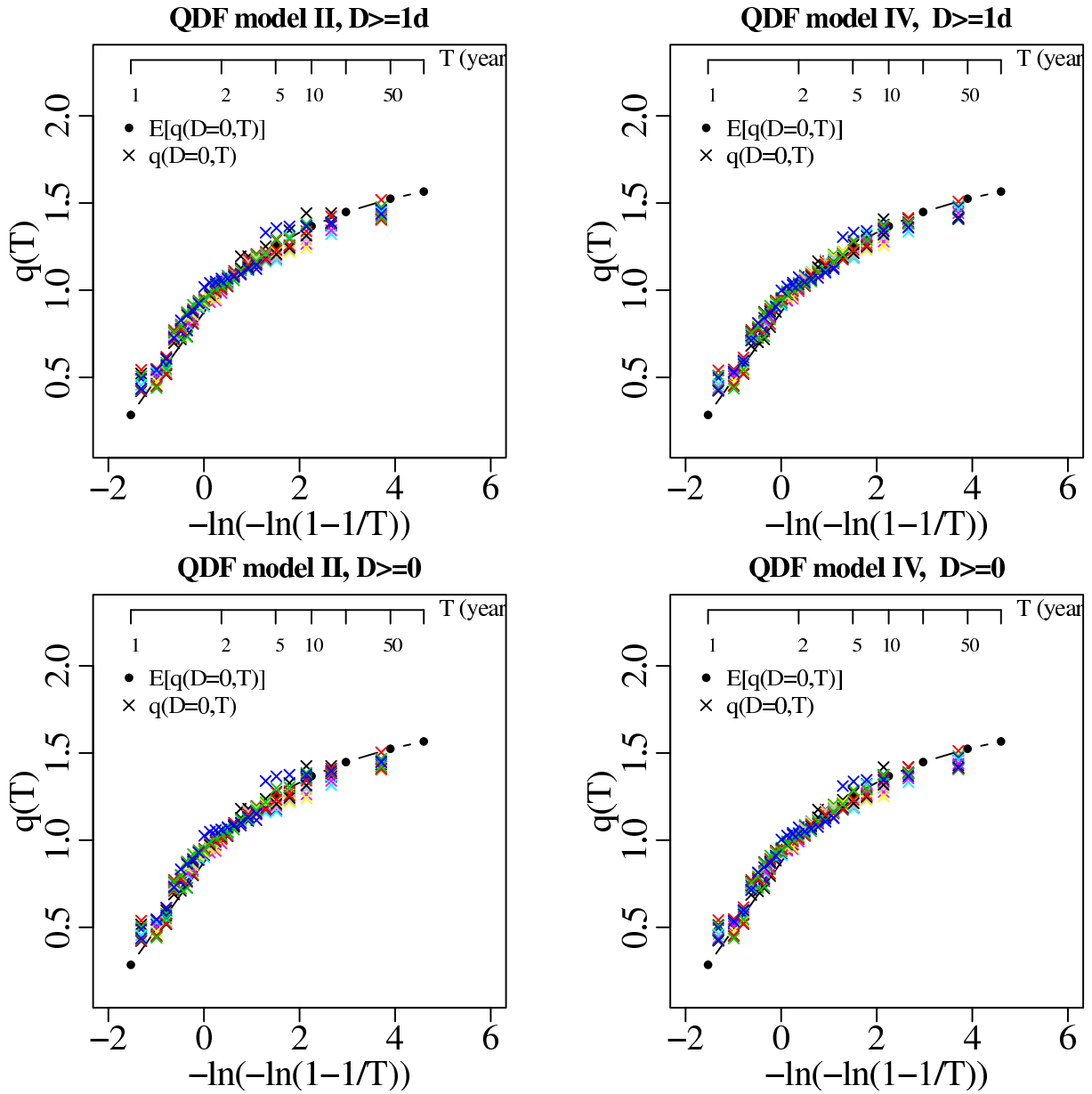


Figure II.5. Estimated dimensionless parent CDF,  $q(T)$ , for basin VHM-45. See caption of fig. II.1.

**Parent distribution  $q(T)$   
VHM 12**

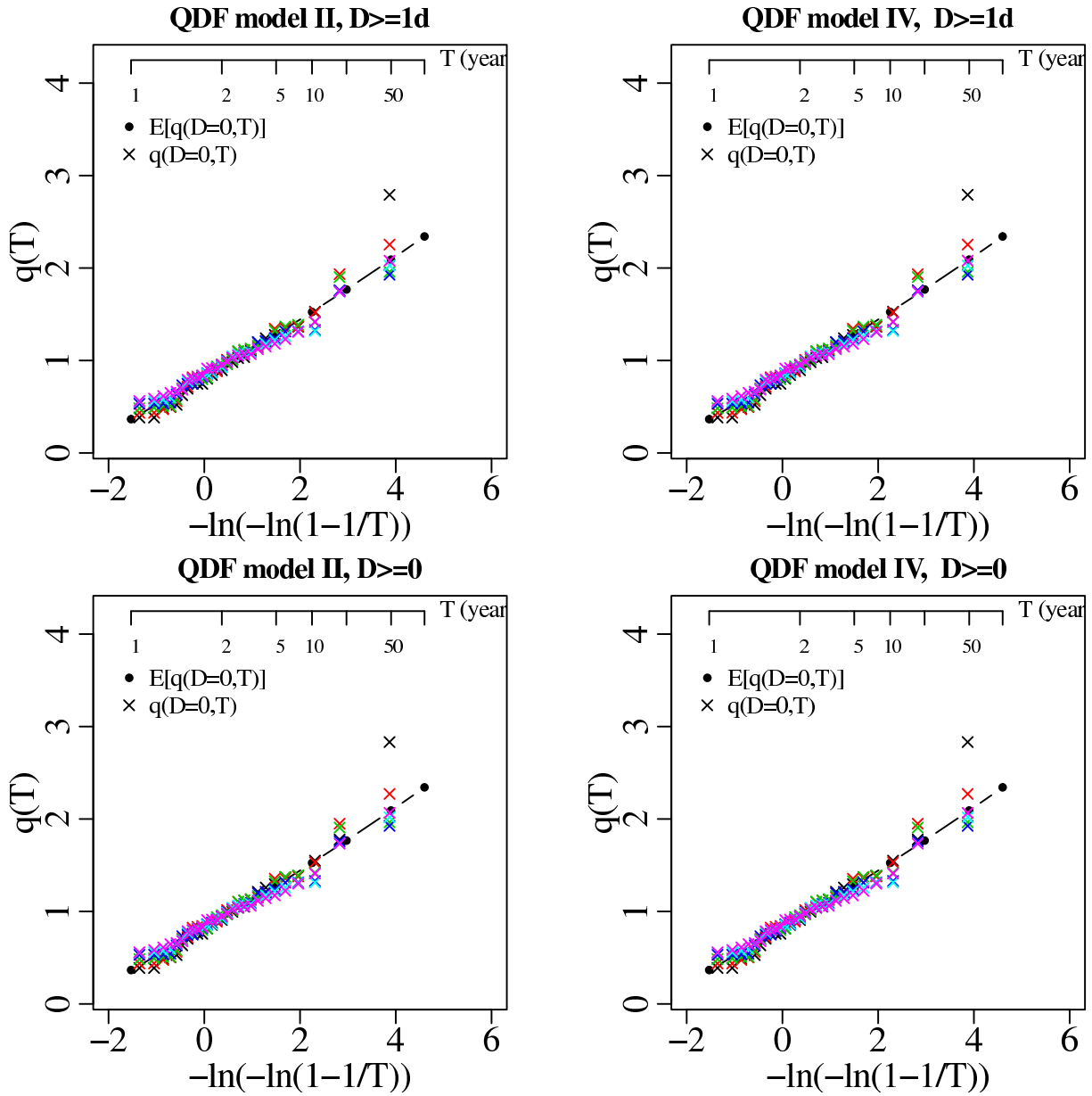


Figure II.6. Estimated dimensionless parent CDF,  $q(T)$ , for basin VHM-12. See caption of fig. II.1.

**Parent distribution  $q(T)$   
VHM 19**

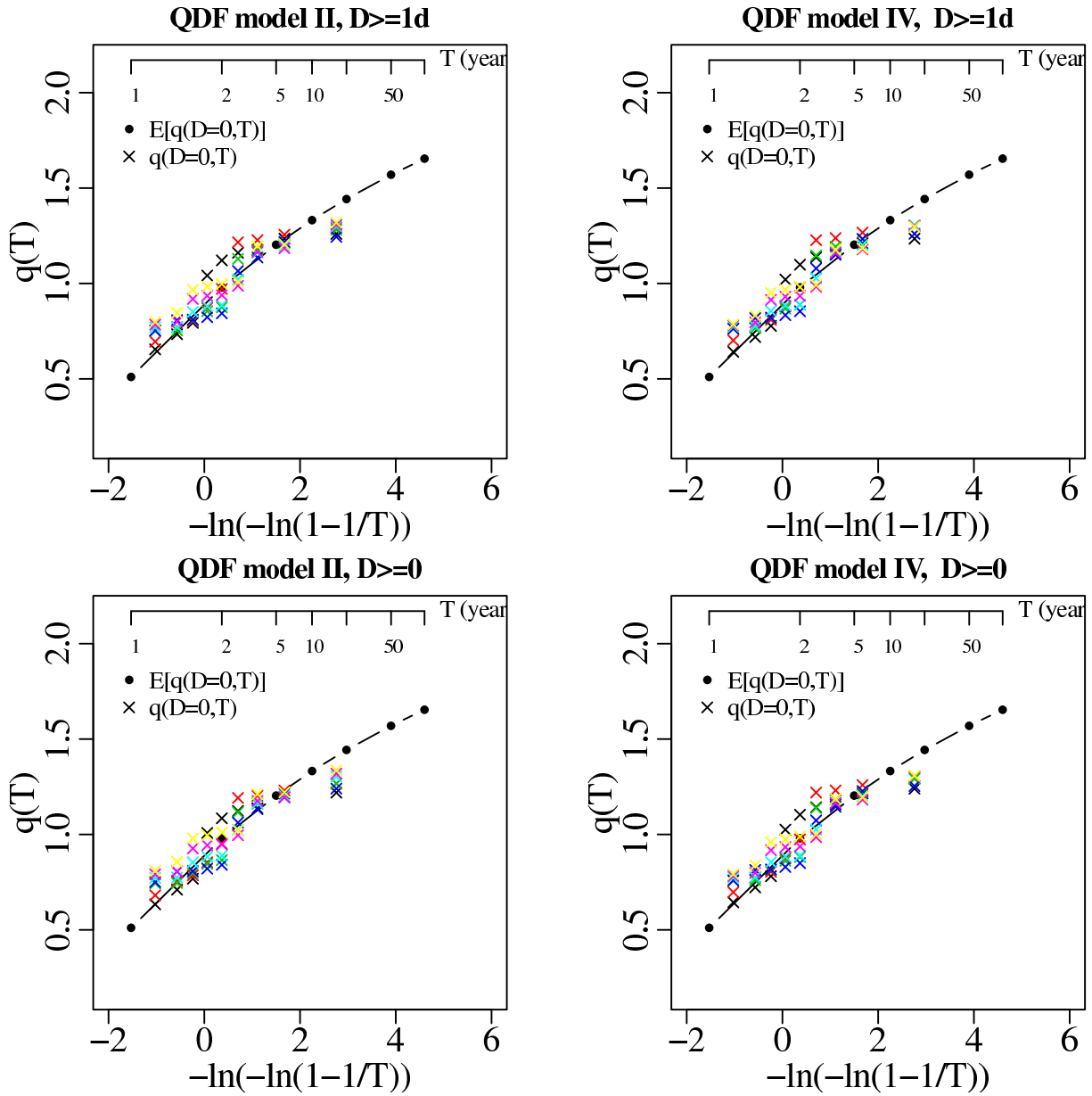
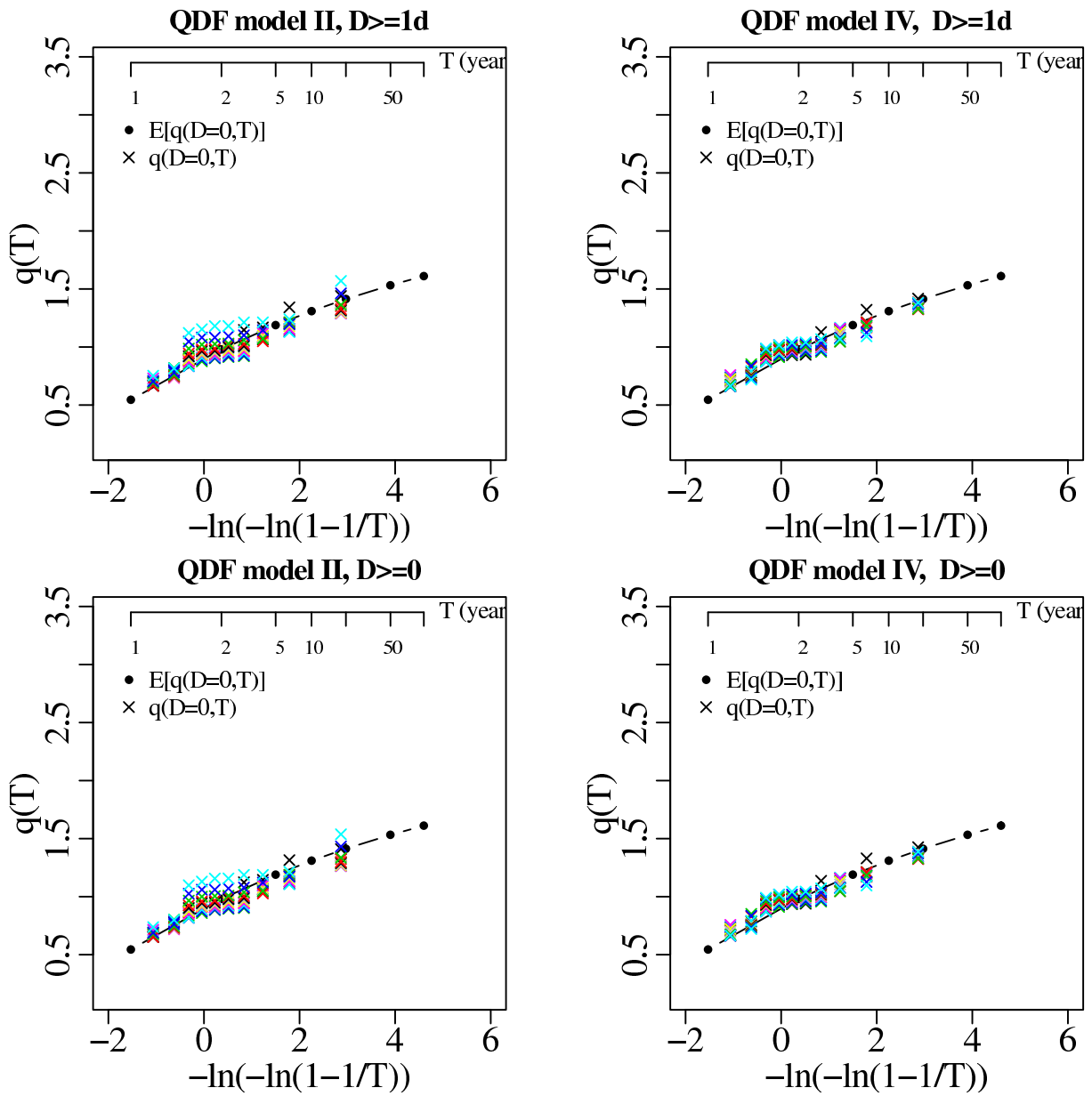


Figure II.7. Estimated dimensionless parent CDF,  $q(T)$ , for basin VHM-19. See caption of fig. II.1.

**Parent distribution  $q(T)$   
VHM 38**



*Figure II.8. Estimated dimensionless parent CDF,  $q(T)$ , for basin VHM-38. See caption of fig. II.1.*



**Parent distribution  $q(T)$   
VHM 198**

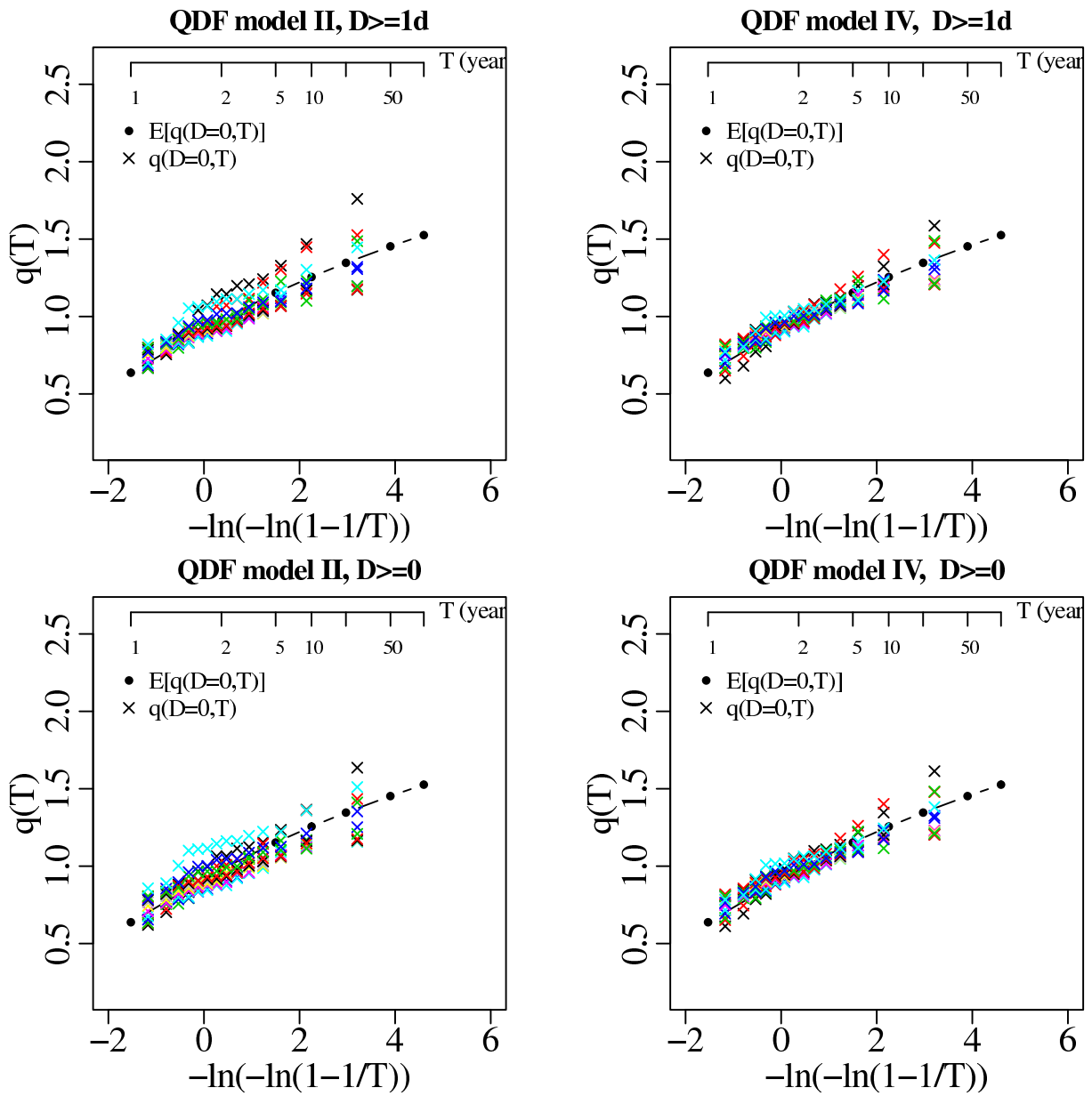


Figure II.9. Estimated dimensionless parent CDF,  $q(T)$ , for basin VHM-198. See caption of fig. II.1.

**Parent distribution  $q(T)$   
VHM 204**

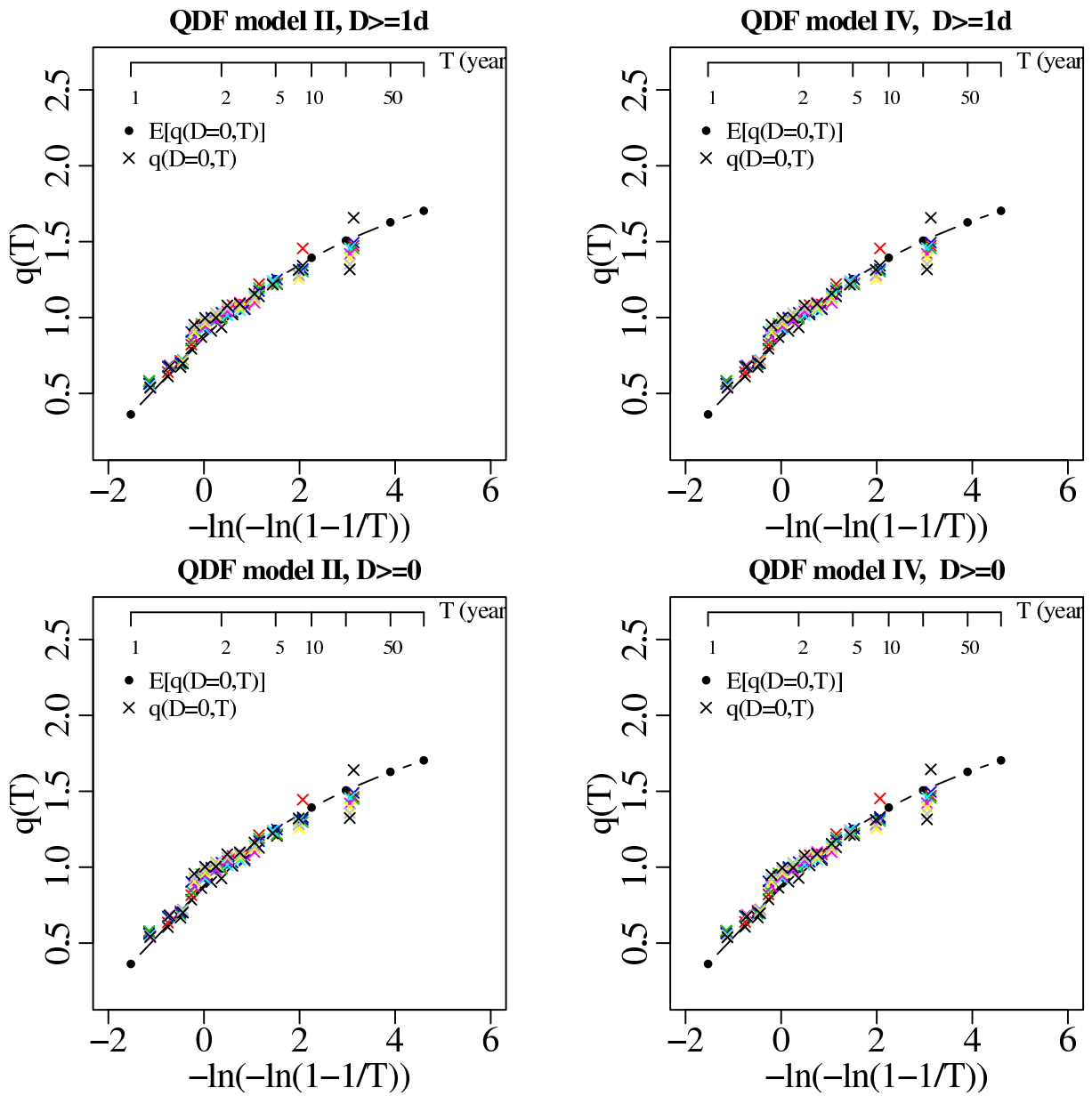


Figure II.10. Estimated dimensionless parent CDF,  $q(T)$ , for basin VHM-204. See caption of fig. II.1.